Antarctic Ice Sheet paleo-constraint database

Benoit S. Lecavalier[1], **Lev Tarasov**[1], **Greg Balco**[2], **Perry Spector**[2], **Claus-Dieter Hillenbrand**[3],
Christo Buizert[4], **Catherine Ritz**[5], **Marion Leduc-Leballeur**[6], **Robert Mulvaney**[3], **Pippa L. Whitehouse**[7],
Michael J. Bentley[7], and **Jonathan Bamber**[8,9]

[1]Department of Physics and Physical Oceanography, Memorial University, St. John's, Canada
[2]Berkeley Geochronology Center, Berkeley, California, USA
[3]British Antarctic Survey, Cambridge, UK
[4]College of Earth, Ocean and Atmospheric Sciences, Oregon State University, Corvallis OR, USA
[5]Université Grenoble Alpes, CNRS, IRD, IGE, Grenoble, France
[6]Institute of Applied Physics National Research Council, Florence, Italy
[7]Department of Geography, Durham University, Durham, UK
[8]Bristol Glaciology Centre, School of Geographical Sciences, University of Bristol, Bristol, UK
[9]Department of Aerospace and Geodesy, Data Science in Earth Observation,
Technical University of Munich, Munich, Germany

Correspondence: Benoit S. Lecavalier (b.lecavalier@mun.ca)

Abstract. We present a database of observational constraints on past Antarctic Ice Sheet changes during the last glacial cycle intended to consolidate the observations that represent our understanding of past Antarctic changes and for state-space estimation and paleo-model calibrations. The database is a major expansion of the initial work of Briggs and Tarasov (2013). It includes new data types and multi-tier data quality assessment. The updated constraint database, AntICE2 (https://theghub.org/resources/4884, Lecavalier et al., 2022), consists of observations of past grounded- and floating-ice-sheet extent, past ice thickness, past relative sea level, borehole temperature profiles, and present-day bedrock displacement rates. In addition to paleo-observations, the present-day ice sheet geometry and surface ice velocities are incorporated to constrain the present-day ice sheet configuration. The method by which the data are curated using explicitly defined criteria is detailed. Moreover, the observational uncertainties are specified. The methodology by which the constraint database can be applied to evaluate a given ice sheet reconstruction is discussed. The implementation of the AntICE2 database for Antarctic Ice Sheet model calibrations will improve Antarctic Ice Sheet predictions during past warm and cold periods and yield more robust paleo-model spin ups for forecasting future ice sheet changes.

1 Introduction

Numerical ice sheet models have been applied to reconstruct past continental-scale ice sheet changes in Antarctica for decades (Whitehouse et al., 2012a; Golledge et al., 2014; Briggs et al., 2014; Huybrechts, 2002; Pollard and DeConto, 2009). However, given the host of uncertainties in such modelling, assessment of the correspondence between model results and past Antarctic Ice Sheet (AIS) evolution requires (among other things) a quality-controlled constraint database

with carefully assessed observational uncertainties. To date, only one database is publicly available (Briggs and Tarasov, 2013), and it suffers from some key limitations. Specifically, many regions, such as in the ice sheet interior, lack any observational constraints, and the data quality was not explicitly evaluated and specified through standardized criteria. Paleo-ice-sheet modelling has a host of uncertainties associated with initial and boundary conditions, physical processes, and their numerical representation. As such, inferences of ice sheet evolution must be meaningfully constrained against

paleo- and present-day (PD) data. This requires an accessible database with well-defined observational uncertainties and a clear understanding of model limitations.

The AIS has consistently been identified as a dominant source of uncertainty in predicting past and future global sea level change (Meredith et al., 2019; Fox-Kemper et al., 2023). Previous studies have generated a wide range of future AIS projections (Little et al., 2013; Levermann et al., 2014; Ritz et al., 2015; Ruckert et al., 2017; Golledge et al., 2015; DeConto and Pollard, 2016) and paleo-retrodictions (Whitehouse et al., 2012a; Golledge et al., 2014; Briggs et al., 2014; Argus et al., 2014; DeConto and Pollard, 2016; Huybrechts, 2002; Simms et al., 2019; Albrecht et al., 2020), often with poorly defined confidence intervals. Most often, these issues are dealt with via parametric tuning to generate reasonable predictions and upper- or lower-bound estimates (e.g. Golledge et al., 2014; DeConto and Pollard, 2016). The integration of a constraint database would help quantify what is deemed a reasonable result. Additionally, most previous studies inadequately explored parametric uncertainties, did not account for structural uncertainties of the model, and only applied a small set of observational constraints. An incomplete uncertainty assessment for model results largely nullifies the utility of the model predictions in the context of understanding the actual physical system under consideration (Tarasov and Goldstein, 2021).

In this study, we provide an overview of a data-quality-curated Antarctic constraint database intended to characterize the past evolution of the AIS and to evaluate and calibrate ice sheet models. Key features are a quality classification and careful specification of data uncertainties. The variety of data types is presented along with spatial and temporal information. A general overview is provided that discusses the data–system relationship and observational uncertainties. In addition, we discuss the future inclusion of additional data types, such as the age structure of the ice, and highlight outstanding issues and community challenges.

2 AntICE2 constraints

The updated community Antarctic Ice Sheet Evolution observational constraint database version 2 (henceforth referred to as AntICE2) builds on the initial work of Briggs and Tarasov (2013) by integrating additional data since the original publication, including new data types. The updated database comprises observations of (1) past grounded-ice and ice shelf extent (paleoEXT), (2) past ice sheet thickness (paleoH), (3) past relative sea level (paleoRSL), (4) borehole temperature profiles (boreTemp), and (5) Global Positioning System (GPS) observations of PD uplift rates (rdotGPS). Figure 1 shows a summary of the data types in the AntICE2 database and their spatial coverage. In addition to these observations, the PD ice sheet geometry (surface elevation, ice thickness, and basal topography; https://nsidc.org/data/ nsidc-0756/versions/3, last access: 6 July 2023) and surface ice velocities (https://nsidc.org/data/nsidc-0484/versions/2, last access: 6 July 2023) are considered. This major revision of the AntICE database more than quintuples the direct observational constraints from 203 to 1023 (excluding the PD AIS geometry and surface velocity field). The database is open source (https://thehub.org/resources/4884, last access: 6 July 2023) and available in the Supplement. The curation of data within the AntICE2 database was based on design criteria that excluded low-quality, inconsistent, and superfluous data. If the inference of past ice sheet changes is not increased when a data point is considered, then it is excluded to prevent database bloating. The curation criteria were established by the collective authorship of this study.

To calibrate or history match a model (Tarasov and Goldstein, 2021), it is necessary to compare model simulations to observations. For such comparison to have meaning, it logically follows that the relationship between each data point and the actual physical system must be specified. The selection of data with a high ratio of signal (measured quantity) to data uncertainty can strongly facilitate the inference process. To calculate a data–model misfit score for a given observation, the observation must include location data (latitude, longitude) and age data determined with a well-established dating technique, and it must quantify the relationship between the proxy observation and the characteristic (i.e. the recorded change in the ice sheet) it constrains. There are many sophisticated approaches to perform a meaningful data–model comparison (Tarasov and Goldstein, 2021), and there are tools that can assist those wanting an initial, albeit limited, data–model comparison implementation (e.g. Ely et al., 2019). For example, past ice thickness inferred from the elevation of an erratic boulder with an age determined by ^{10}Be cosmogenic-nuclide exposure dating constrains the time when ice sheet thinning caused the ice surface to fall below the altitude of the sample. The paleo-data are categorized by site, where data from nearby samples (typically within < 10 km distance) are clustered together, thereby yielding a time series at a given site (paleoRSL, paleoH). The exact spatial coordinates of the data are taken from the source publication and transcribed into the database. The sites of the paleo-data in Figs. 1 and 2 show the average location of all the data clusters near a given site.

Each site has a unique four-digit identifier (Fig. 2). The first digit represents the data type (paleoH = 1, paleoEXT = 2, paleoRSL = 9, boreTemp = 5, and rdotGPS = 8), the second digit designates the drainage basin sector (Dronning Maud Land–Enderby Land = 1, Lambert–Amery = 2, Wilkes–Victoria Land = 3, Ross Sea = 4, Amundsen Sea and Bellingshausen Sea = 5, Antarctic Peninsula = 6, and Weddell Sea = 7; sector boundaries are shown in Fig. 2), and the last two digits identify the site within each sector (westernmost site = 1, increasing by 1 eastward following the coast). The types of paleo-data along with full references are found
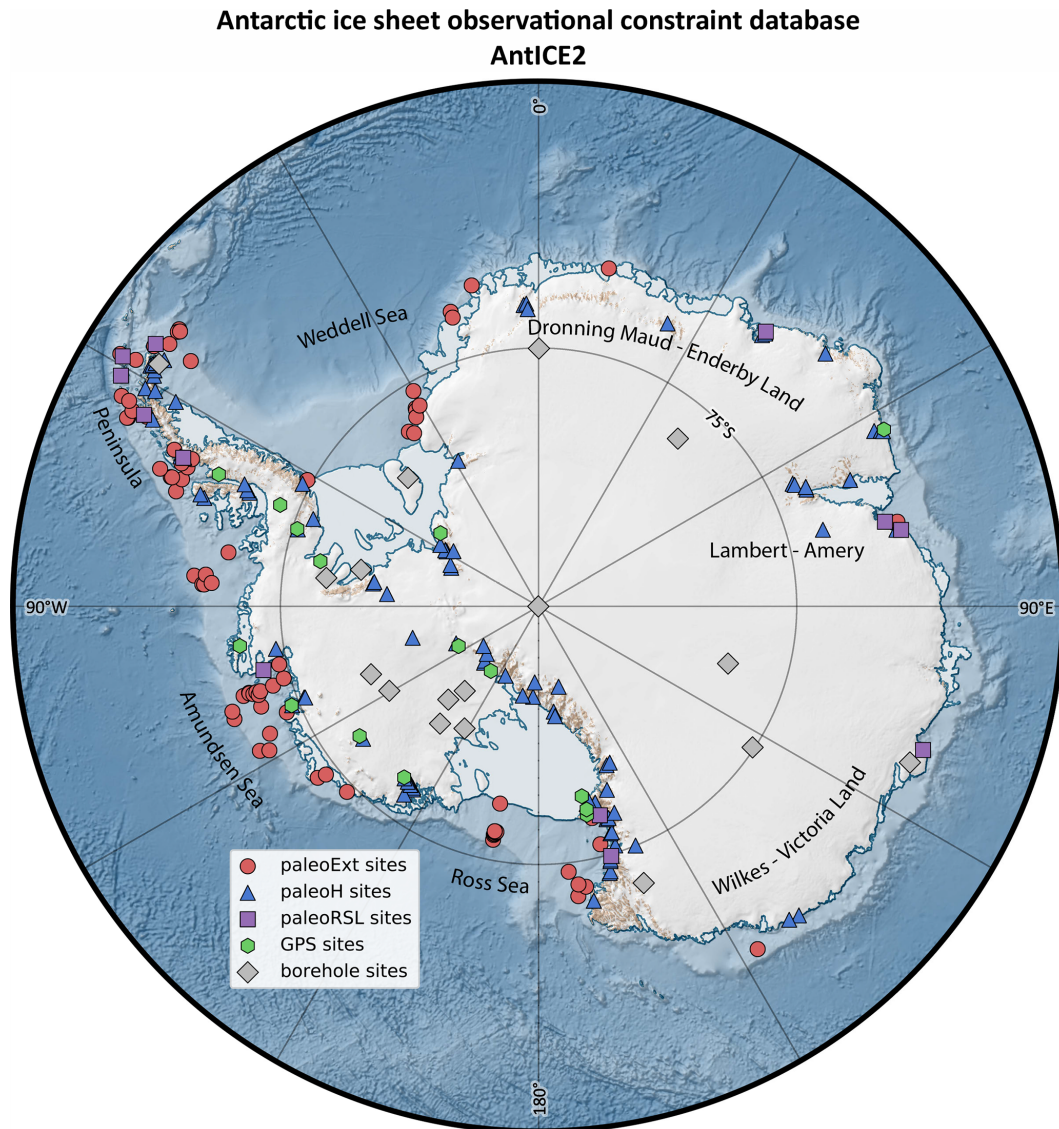
Figure 1. Antarctic Ice Sheet Evolution database version 2 (AntICE2) summary plot. The Antarctic basemap was generated using Quantarctica (Matsuoka et al., 2021).

in Tables S1–S5 in the Supplement. The method by which the data is processed and interpreted is described below.

2.1 Paleo-ice-sheet thickness

When an ice sheet recedes and thins, entrained terrigenous detritus in the ice is deposited on newly exposed land. The geographic coordinates, elevation, and exposure age of the bedrock or erratic sample provide a point estimate of the location of the ice surface or margin at the time of exposure. Note that, while the measured elevation is relative to PD sea level, the elevation at the time of initial exposure is unknown without knowledge of the glacial isostatic adjustment (GIA) history. However, the GIA estimate is not needed if the measurement is treated as a direct constraint on past ice thick-

ness rather than ice surface elevation. In Antarctica, these measurements are mostly conducted along the slope of ice-free mountains or nunataks piercing through the ice sheet surface (e.g. Balco et al., 2016; Small et al., 2019). When many samples along a transect across a topographical slope are analysed, one can reconstruct a chronology of paleo-ice-sheet thinning since the last ice thickness maximum in the region (Stone et al., 2003; Ackert et al., 2007). This is illustrated in Fig. 3, showing sample elevation histories from different sites during the deglaciation following the Last Glacial Maximum (LGM: ca. 19–23 ka) and in Figs. S1–S102 in the Supplement, showing the entire AntICE2 paleoH dataset.

Cosmogenic-nuclide exposure dating on bedrock and erratics is the primary method used to establish the timing of deglaciation of terrestrial sites (Bentley et al., 2006; John-
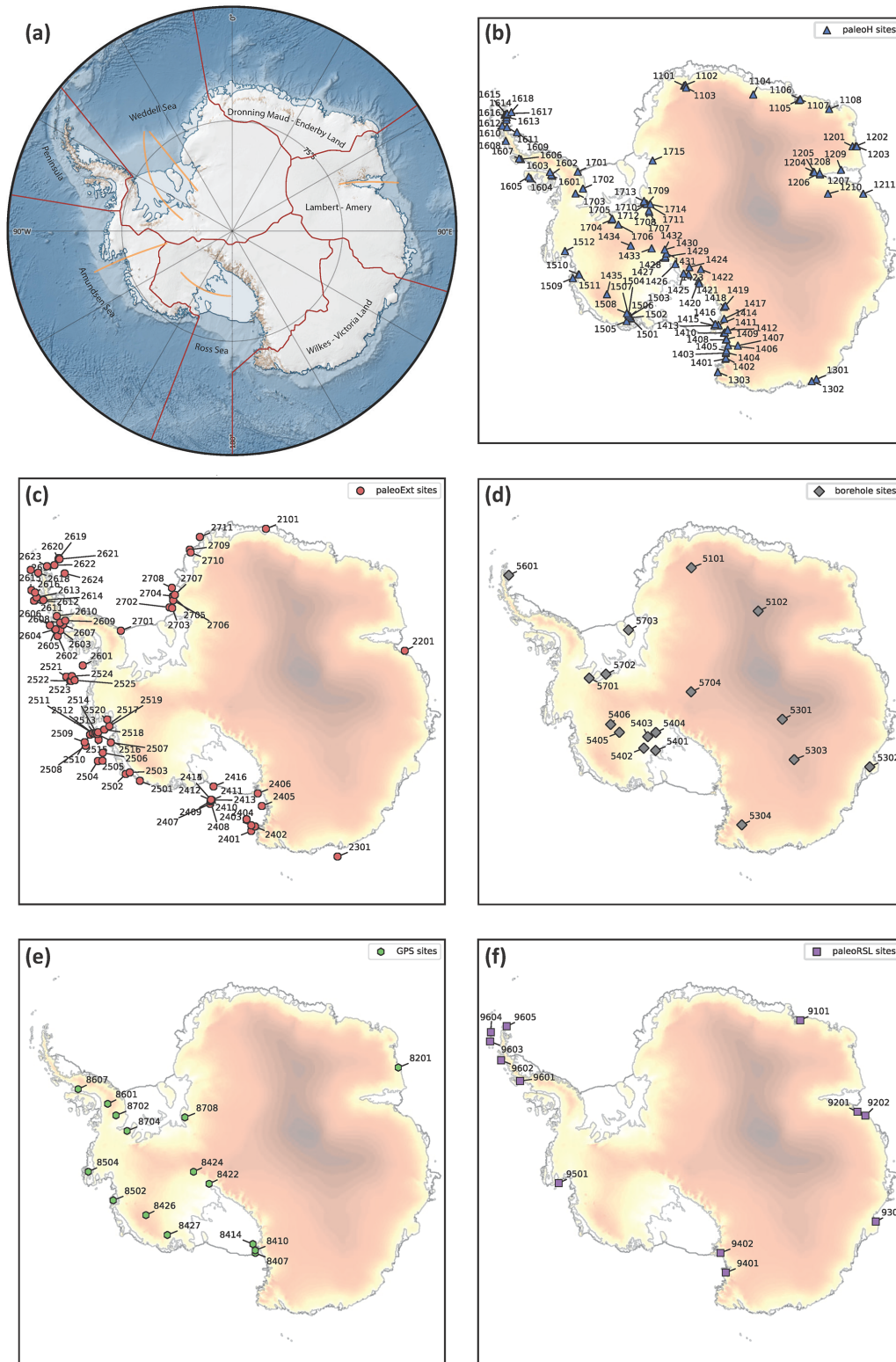
Figure 2. (a) Clustered IMBIE2 ice drainage basins (boundaries between clusters marked by red lines), key cross-section profiles (orange lines), and place names mentioned in the text; **(b–f)** are the sites with past ice thickness data (paleoH), past ice extent data (paleoExt), ice core borehole temperature profiles (boreTemp), present-day uplift rates (rdotGPS), and past relative sea level data (paleoRSL), respectively. The basemap shown in **(a)** was generated using Quantarctica (Matsuoka et al., 2021). The surface elevation shown in **(b–f)** is based on the BedMachine Antarctica version 2 dataset (Morlighem et al., 2020).
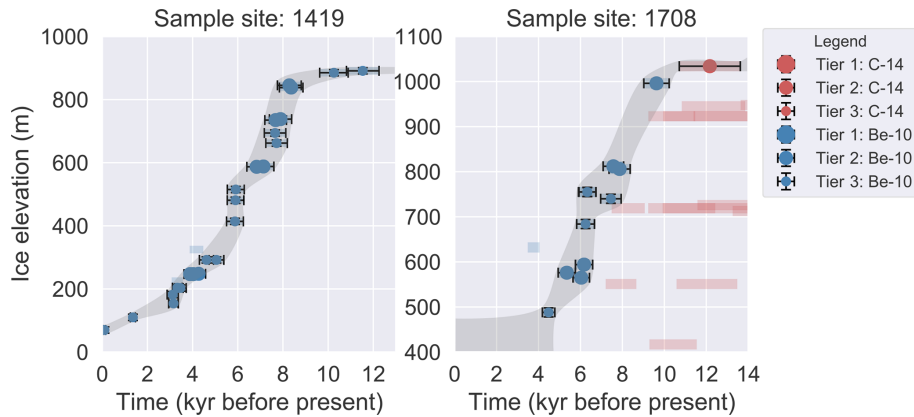
Figure 3. Sample past ice thickness (paleoH) data to illustrate the data quality and tier assignment. The elevation data are converted to ice thickness data using the BedMachine basal topography data. The grey band illustrates the expert-assessed 2σ bounds on history at the given site. The blue and red transparent bands represent other C-14 and Be-10 data not assigned to a quality tier.

son et al., 2017; Nichols et al., 2019). The method entails the measurement of radioactive- and stable-nuclide isotopic concentrations (^{10}Be, ^{26}Al, ^{3}He, ^{21}Ne, ^{36}Cl, and ^{14}C) which accumulate in rock surfaces exposed to the atmosphere and therefore to the cosmic-ray flux. In the case of these isotopes, the nuclide concentration builds up when a rock exposed to the atmosphere is bombarded by cosmic rays (Ackert et al., 1999, 2007; Stone et al., 2003). Using the nuclide concentration and its radioactive half-life, the time when a rock was first exposed to cosmic rays, i.e. its exposure age, and thus the deglaciation age of its location can be calculated.

The interpretation of the deglaciation age can be complicated when erratics are absent or were redeposited (e.g. down a mountain slope); when the dated bedrock surface has been sufficiently eroded to remove cosmogenic nuclides accumulated during prior exposure periods; and/or when the site has subsequently been reburied by ice, snow, or sediment or shielded by topography. In a case where the cosmogenic nuclide clock was not sufficiently reset and thus where past nuclide concentrations persist, the sample would suffer from significant inheritance of pre-ice-cover exposure to cosmic rays. Given the limited number of areas in Antarctica where bedrock or erratics are exposed today, the total resulting number of collected samples is relatively low. This makes it difficult to identify when inheritance is an issue unless significant sample numbers are collected or paired ^{10}Be–^{26}Al dating is performed. For a complete description of the cosmogenic-nuclide-exposure-dating methodology and its challenges, we refer the reader to previous studies (Ackert et al., 1999; Stone et al., 2003; Bentley et al., 2006; Mackintosh et al., 2007; Balco et al., 2016; Johnson et al., 2017).

An informal cosmogenic-nuclide exposure age database (ICE-D) already exists and facilitates accessibility to raw data and derived exposure ages. The ICE-D database (https://www.ice-d.org/, last access: 6 July 2023) is inclusive and illustrates the conflicting and complex exposure histories in many regions. Quality control and processing of the data are required since many samples suffer from inheritance, and some regions provide an inconsistent record of past ice surface lowering (younger samples being higher than older samples). The deglaciation age is often inferred by the highest and youngest erratic sample (Bentley et al., 2006), with older bedrock samples at a similar elevation being discounted. Alternatively, a mean age of several samples for a site may be calculated (Todd et al., 2010). In the original AntICE database (Briggs and Tarasov, 2013), the exposure ages and uncertainties were taken directly from the literature rather than recalibrating the ages for overall consistency, in part because the raw data were often inaccessible. The ICE-D database addresses this issue by using a single, up-to-date method to calculate all cosmogenic-nuclide exposure ages. Exposure ages used in this compilation were calculated using the LSDn scaling method of Lifton et al. (2014), as implemented in version 3 of the online exposure age calculator described by Balco et al. (2008) and subsequently updated by Balco (2020). Production rate calibration for ^{3}He in pyroxene and olivine, ^{10}Be in quartz, and ^{26}Al in quartz uses the primary calibration datasets of Borchers et al. (2016). Production rate calibration for in situ ^{14}C is based on measurements of the CRONUS-A quartz standard and the assumption that the concentration in this sample is at production–decay saturation, as described in Nichols et al. (2019). An altitude uncertainty value of ±10 m is imposed when source publications do not include elevation uncertainty estimates. Whenever information on uncertainties is lacking in the source publication, uncertainty estimates are judged conservatively by relevant expert members of the author team or are derived from other studies using the same data type. The past ice thickness site IDs and locations are shown in Fig. 2 and visualized on a site-by-site basis in Figs. S1–S102 in the Supplement.

Samples dated using in-situ-produced radiocarbon were previously not incorporated in the paleo-AIS thickness database. Because of the short half-life of ^{14}C, this method is largely insensitive to inheritance on the deglacial timescales of interest and can therefore help identify cosmogenic nuclide exposure ages unbiased by inheritance. Consequently, in situ ^{14}C dating has resolved inconsistencies in AIS reconstructions for the Weddell Sea drainage sector (e.g. 1701, 1713, and 1715), where prior cosmogenic-nuclide exposure dating suggested hundreds of metres of thinning since the LGM, with neighbouring sites indicating no elevation changes relative to present during the same time period (Nichols et al., 2019). The inclusion of in situ radiocarbon data from the Shackleton Range, Lassiter Coast, and Schmidt Hills has increased consistency among paleo-ice-thickness data. Since the LGM, the revised data indicate that the Weddell Sea sector experienced a lowering of the ice sheet surface of ~ 300 to 600 m, with a few sites exceeding 800 m of lowering (Balco et al., 2016; Hein et al., 2016; Bentley et al., 2010, 2017; Johnson et al., 2019; Nichols et al., 2019); this largely reconciles contradictory reconstructions of the regional post-LGM glacial history based on marine and terrestrial records (Hillenbrand et al., 2014).

New exposure data from the Transantarctic Mountains along the Ross Sea embayment tell a more complete, albeit only local, post-LGM ice-sheet-thinning history for the mountain chain. During the LGM, the surfaces of outlet glaciers presently draining directly into the Ross Sea reached an elevation of 260 to 550 m above today (e.g. Jones et al., 2015; Balco et al., 2019). Of the other outlet glaciers feeding the LGM Ross Ice Shelf and Sheet system, several had an elevation of ~ 1000 m above today during the LGM (Spector et al., 2017). Paleo-ice-thickness data adjacent to the Siple Coast and Ross Island, as originally compiled in the AntICE database, showed that the ice sheet surface elevation at the onset of the post-LGM deglaciation ranged from ~ 1000 to 2000 m above present. This illustrates the regional variability along the Transantarctic Mountains, with greater potential LGM elevation changes recorded further south and with significant variance among the sites likely being related to local topographical features of specific valleys (Stone et al., 2003; Todd et al., 2010; Storey et al., 2010).

The Amundsen Sea drainage sector in West Antarctica has limited outcrops suitable for exposure dating; therefore, the region's past ice thickness is poorly constrained. The original database had a total of five data points constraining the elevation of the ice sheet surface at the LGM and at the start of the Holocene (11.7 ka) in the hinterland of the Amundsen Sea embayment to be between 45 and 300 m above present (Ackert et al., 1999; Johnson et al., 2008). New cosmogenic exposure ages, totalling 25 quality exposure ages, suggest a pre-Holocene ice elevation upwards of at least 330–560 m above present (Johnson et al., 2017, 2020). In the original version of the AntICE database, the Antarctic Peninsula lacked any paleo-ice-thickness data. Three new histories are included in

our new iteration, and they all consistently report an ice elevation of ~ 350 m above present early in the last deglaciation (Johnson et al., 2019; Bentley et al., 2011; Balco and Schaefer, 2013; Glasser et al., 2014). Finally, a new thinning history from the Sør Rondane Mountains in Dronning Maud Land proposes an ice surface lowering of less than 50 m during the last deglaciation (Suganuma et al., 2014).

In our study here, we also include previously unpublished exposure data constraining AIS thinning since the last glacial period (Figs. S41, S44, S47, S63 in the Supplement). This includes some newer data of high quality (e.g. 1419, 1422, 1425, and 1506) that are not yet published in peer-reviewed articles but are included in the ICE-D database due to public-access requirements of funding agencies.

2.2   Paleo-ice-sheet extent

The stratigraphy of marine sediment cores from the Antarctic continental shelf can preserve some of the complex history of glacial advance and retreat (Smith et al., 2019). The retreat of the grounding line (GL) can be inferred from the stratigraphic succession from subglacial to GL-proximal glacimarine sediments and that of the calving line can be inferred from the transition of GL-distal glacimarine to seasonal open-marine deposits (Smith et al., 2011; Anderson et al., 2014; Arndt et al., 2017; Bart et al., 2017; Heroy and Anderson, 2007).

Dating the transition from subglacial to glacimarine facies provides the age of the GL retreat across a core site, but usually, this approach has to rely on ^{14}C dating of biogenic material. ^{14}C dates obtained from calcareous (micro-)fossils provide the most robust age constraints for Antarctic marine sediments (e.g., Domack et al., 2005). However, there is a paucity of biogenic carbonate in Antarctic shelf sediments in general and in the GL-proximal facies directly overlying the subglacial till in particular. As such, either calcareous fossils (if present) from the open-marine facies or organic matter from the GL-proximal facies have to be dated (Bart et al., 2017). While the former dates only provide an absolute minimum age for GL retreat from a core site, the latter dating approach is hampered by the fact that the organic matter content in GL-proximal facies is typically very low and that this organic material often comprises large amounts of subglacially reworked fossil organic carbon. This can result in ^{14}C ages much older than the time of sediment deposition and, thus, the time of GL retreat (Licht et al., 1998; Domack et al., 1999; Pudsey et al., 2006; Heroy and Anderson, 2007). Over the past 2 decades, some progress has been made in (i) assessing the reliability of organic-matter-based ^{14}C ages in constraining GL retreat (Hillenbrand et al., 2010a; Smith et al., 2014); (ii) compound-specific ^{14}C dating of only the young, fresh fraction of the organic material (Ohkouchi and Eglinton, 2008; Rosenheim et al., 2008; Yokoyama et al., 2016; Subt et al., 2017); (iii) obtaining reliable ^{14}C ages from even very small amounts of biogenic carbonate (Klages et

al., 2014; Arndt et al., 2017, 2020); and (iv) utilizing paleomagnetic methods for dating Antarctic sediment cores (Hillenbrand et al., 2010b; Smith et al., 2021).

Retreat of the calving line of an ice shelf is usually reflected in a sediment core from the Antarctic shelf by means of the transition from a fine-grained terrigenous facies deposited distally from the GL into a biogenic-bearing, often diatom-rich facies deposited under open-marine conditions (Livingstone et al., 2012; Yokoyama et al., 2016; Bart et al., 2017). However, research on modern sub-ice-shelf environments has shown that ocean currents can advect biogenic material from open-ocean settings far under ice shelves, where they can sustain benthic fauna assemblages and potentially result in deposition of sediments resembling open-marine facies (Hemer and Harris, 2003; Hemer et al., 2007; Post et al., 2007; Riddle et al., 2007). Measurements of the cosmogenic-nuclide ^{10}Be in marine shelf sediments has shown promise that this ambiguity can be avoided in future studies (Yokoyama et al., 2016). Thus, despite all the aforementioned improvements, the dating of Antarctic shelf sediments and constraint of the time of GL and calving-line retreat still remain a challenge.

The combination of the complex stratigraphy of sediment cores from the Antarctic continental shelf and the lack of reliable age control for key facies renders the interpretation of the proxy record in most cores non-trivial. For this reason, only those marine sediment records that clearly document a position below grounded ice, under an ice shelf, or in (seasonal) open water at a particular time are added to the AntICE2 database (Figs. 4 and S104–S180 in the Supplement).

The paleoEXT database was originally a curated version of the GL retreat ages compiled by Livingstone et al. (2012). Our new iteration has been updated to include the RAISED consortium compilation (Bentley et al., 2014; Hillenbrand et al., 2014; Anderson et al., 2014; Mackintosh et al., 2014; Ó Cofaigh et al., 2014; Larter et al., 2014), and it has also been supplemented by a number of more recent studies (Bart et al., 2018). For each marine sediment core, obvious ^{14}C age outliers or down-core age reversals, if present, were removed in accordance with the source literature. Converting measured radiocarbon activities to calendar age requires corrections for the variable atmospheric radiocarbon history and for the reservoir age of the ocean. All the past ice extent ages were recalibrated using a consistent marine reservoir correction of 1144 ± 120 yr (Hall et al., 2010) with CALIB v8.1 (CALIB rev. 8; Stuiver and Reimer, 1993) using the Marine20 calibration curve (Heaton et al., 2020). The full information for the marine cores, including expedition ID, sample depth, etc., is given in the ICE-D marine database (http://marine.antarctica.ice-d.org/, last access: 21 December 2023).

Since the original AntICE database, numerous cruises have collected marine sediment cores along transects from near the modern ice shelf front to the continental-shelf edge. The biggest addition of data occurred in the Amundsen Sea

sector, where LGM grounded-ice extent and deglacial GL retreat have been reconstructed across Pine Island–Thwaites Trough (Smith et al., 2014; Hillenbrand et al., 2013; Kirshner et al., 2012), Dotson-Getz Trough (Smith et al., 2011; Hillenbrand et al., 2010b), Abbot–Cosgrove Trough (Klages et al., 2017), and Hobbs Trough (Klages et al., 2014). In Pine Island–Thwaites Trough, the initial GL retreat from the outer continental shelf occurred at 20 ka, reaching the middle shelf by 13.6 ka and the inner shelf by 10.6 ka (Larter et al., 2014; Smith et al., 2014). In the Ross Sea sector, marine sediment cores indicate an initial retreat from the continental-shelf edge prior to the Holocene. The Holocene retreat across large sections of the eastern and western Ross Sea continental shelf was asynchronous (Anderson et al., 2014; Bart et al., 2018) but occurred during the early to middle Holocone (McKay et al., 2008, 2016; McGlannan et al., 2017; Bart et al., 2018). The calving line of the Ross Ice Shelf retreated throughout the middle to late Holocene, reaching its present extent by ~ 1.5 ka (Yokoyama et al., 2016). In the Weddell Sea, cores from the outer Filchner Trough suggest that the GL advanced and retreated prior to the LGM and readvanced again in the early Holocene before retreating by 8.7 ka (Stolldorf et al., 2012; Arndt et al., 2017). These additional paleo-ice-extent data portray a regionally complex deglacial history (Arndt et al., 2017, 2020; Hodgson et al., 2018).

2.3 Paleo relative sea level

Reconstructions of past sea level are based on a variety of indicators: isolation basins; raised beaches and deltas; marine shells; driftwood; whale, seal, and penguin fossils; bedrock exposure dating; and lower elevational limits of perched boulders (Verleyen et al., 2005, 2017; Shennan et al., 2015; Hodgson et al., 2016). The dated relative-sea-level (RSL) proxy data infer an upper bound, a lower bound, or a two-way bounded estimate on past sea level given the height of the datum relative to present sea level. Geographically proximal data form a local RSL history which constrains sea level change through time. Only 0.44 % of Antarctica is ice-free land, which limits the regions where past sea level records can be investigated, and many of these outcrops are nunataks at high altitudes (Hodgson et al., 2016; Verleyen et al., 2017). For the Antarctic domain, the most common RSL data are based on records of raised beaches, isolation basins, molluscs, and penguin remains.

The sea level proxy data with the highest accuracy are those from isolation basins, which originally formed as marine basins but became subsequently isolated from the ocean through sea level fall and/or glacial isostatic rebound of the bedrock (NB: an isolation basin can later be reconnected to the ocean by subsidence and/or sea level rise). The sill height that controls drainage from the basin is the RSL elevation proxy. Dating the microfossil remains at the marine–lacustrine or lacustrine–marine transition of a sediment core extracted from an isolation basin determines the age of iso-
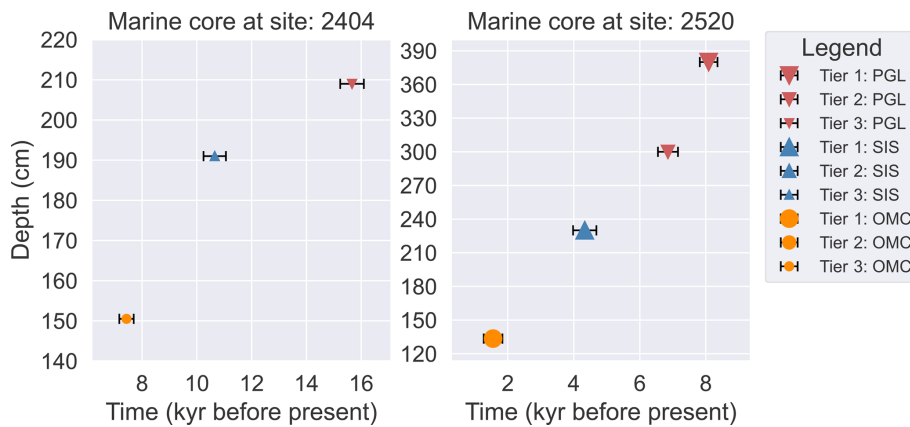
Figure 4. Sample past ice extent (paleoExt – proximal to the grounding line, PGL; sub-ice-shelf, SIS; open-marine conditions, OMC) data from a marine sediment core to illustrate the data quality and tier assignment.

lation from or reconnection to the ocean. Together, this establishes a precise RSL elevation and age for a given site (Zwartz et al., 1998; Verleyen et al., 2005; Roberts et al., 2011). Past RSL observations of lesser quality that simply constrain a maximum or minimum elevation of past sea level come from ^{14}C ages on biogenic material buried in raised beaches. Dates on mollusc shells or penguin fossils provide an age for the paleo-beach (Hall and Denton, 1999; Shennan et al., 2015). Similarly, burial ages of raised beaches can be derived from optically stimulated luminescence (OSL) dating of beach cobbles (Simkins et al., 2013). Additional details on the RSL proxy data are discussed in Briggs and Tarasov (2013).

The AntICE2 past RSL sites and their IDs are shown in Fig. 2 and visualized in Figs. 5 and S181–S192 in the Supplement. When uncertainties were provided in the source publications, they were incorporated in the database. When they were lacking, a ±1 m elevation uncertainty was assumed. Moreover, as in Briggs and Tarasov (2013), another ±1 m uncertainty is added to allow for present and paleo tidal variations (Sun et al., 2022) when measured uncertainties are less than 2 m. The radiocarbon ages in the database were recalibrated using the CALIB v8.1 with the IntCal20 (SHCal20), Marine20, or the mixed marine Southern Hemisphere radiocarbon calibration curve depending on the sample type and content of marine material (Reimer et al., 2009; Heaton et al., 2020). The source publications use different marine reservoir corrections depending on the dated material, while our database standardizes the marine reservoir correction to 1144 ± 120 yr (Hall et al., 2010) for simplicity and consistency. By providing the uncorrected ^{14}C ages, uncertainties, and marine reservoir corrections, the relative-sea-level dataset can easily be recalibrated. Moreover, this enables the data to be incorporated within an online database (e.g. ICE-D RSL repository) so that ages can be dynamically recalibrated upon request.

The additional RSL data in the AntICE2 database have significantly increased the geographic coverage when compared to the original iteration (Simms et al., 2011; Simkins et al., 2013; Hodgson et al., 2016; Verleyen et al., 2017). In Dronning Maud Land, new isolation basin data from Lützow-Holm Bay more robustly constrain past RSL, which is estimated to have fallen by 20 m over the Holocene (Verleyen et al., 2017). These sea level index points are generally consistent with the previously published limiting dates (Miura et al., 1998). The Lambert–Amery sector around Prydz Bay contains exposed coastal land, where isolation basin contacts, shells, and penguin fossils from raised beaches were dated (Hodgson et al., 2016). This has boosted the reconstructed sea level history of the region, suggesting an early Holocene sea level rise from a −4 to +8 m highstand at ∼ 8 ka, subsequently followed by a gradual fall to PD levels starting at ∼ 8 ka (Zwartz et al., 1998; Berg et al., 2010; Hodgson et al., 2016). In the Amundsen Sea sector, there is one ^{10}Be exposure date potentially constraining sea level change from a sample that is suspected to have experienced isostatic emergence from the ocean at 2.2 ka (Johnson et al., 2008). Alternatively, this exposure date with a modern elevation of 8 m above sea level could simply reflect ice margin retreat. The Antarctic Peninsula is constrained by six RSL time series. Marguerite Bay provides limiting dates and a few isolation basin ages that indicate a ∼ 20 m sea level fall from 7 ka, reaching PD sea levels by 1.5 ka (Emslie and McDaniel, 2002; Bentley et al., 2005; Simkins et al., 2013). The South Shetland Islands contain some of the largest ice-free sections of land in Antarctica, providing upper and lower bounds on past sea level and, more importantly, isolation basin index data which imply a sea level fall from a 16 m highstand at ∼ 8 ka (Watcham et al., 2011; Simms et al., 2011). Near and on James Ross Island, isolation basin index data indicate a gradual Holocene sea level fall, with the earliest constraint indicating that sea level was 11 m above present at 6 ka (Hjort et al., 1997; Roberts et al., 2011).
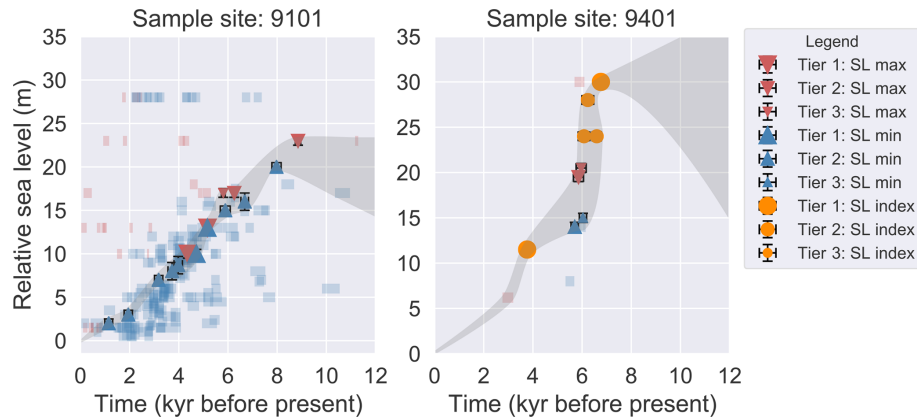
Figure 5. Sample past relative sea level (paleoRSL) data to illustrate the data quality and tier assignment. The grey band illustrates the expert-assessed 2σ bounds on history at the given site. The transparent blue and red bands represent other limiting ages not assigned to a quality tier.

2.4 Ice core borehole temperatures

The original AntICE database lacked constraints in the interior of the ice sheet. To partly remedy this major issue, we incorporate a new powerful data type – the temperature profiles of major Antarctic ice core boreholes (Fig. 6). The temperature structure of the ice can be measured by running a temperature logger down the borehole of an ice core (Cuffey et al., 2016). Past changes in temperature, ice velocity, and ice thickness will affect the thermal structure of the ice sheet. Therefore, the resulting observations of temperatures through the ice constrain the present and past thermal forcing and ice dynamics.

Borehole temperature profiles generally have one of two structures characterized by the depth of the englacial thermal minimum. In the first case, a borehole temperature profile is characterized by minimum temperatures near the ice surface which progressively increase towards the bed (Engelhardt, 2004a, c; Motoyama, 2007; Lukin and Vasiliev, 2014; Weikusat et al., 2017; Mulvaney et al., 2021; Buizert et al., 2021); this case is typical of low-accumulation sites dominated by heat diffusion. In the second case, ice temperatures remain cold at depth and reach a deeper englacial thermal minimum, which is marginally cooler than the surface ice, before they warm again towards the base, such as at the sites of the West Antarctic Ice Sheet Divide ice core (WDC) and Byrd ice core (Gow et al., 1968; Van Ommen et al., 1999; Cuffey et al., 2016); this case is typical of high-accumulation sites dominated by the downward advection of cold surface ice. The ice thickness, geothermal heat flux, horizontal ice advection, and surface accumulation are the main controls on whether or not the base is at the pressure-melting point, with serious ramifications for basal hydrology and ice dynamics.

The various borehole temperature profiles were measured using different instruments, and some were measured at a time considerably after the ice core had been drilled (Motoyama, 2007; Lukin and Vasiliev, 2014). With the precision

of the used temperature logger rarely reported in a source publication, an uncertainty value of $\pm 0.1\,°C$ is assumed. The Talos Dome and South Pole borehole temperature profiles do not cover the majority of the entire ice column, minimizing their overall constraint effectiveness capability. Several borehole temperature profiles have been measured along the Siple Coast in the Ross Sea sector (Engelhardt, 2004a). Although they all share a high degree of correlation, a total of four Siple Coast boreholes were included in the database to maximize both the spatial distribution and the number of prominent ice sheet features sampled. The temperature profiles are from the Siple Dome, Bindschadler, Kamb, and Alley–Whillans ice stream boreholes (Engelhardt, 2004a, b).

2.5 Present-day uplift vertical land motion

Across Antarctica, a Global Positioning System (GPS) network measures the displacement of the solid Earth. GPS measurements, although relatively scarce, can supplement the even-sparser RSL dataset in constraining the isostatic response of the solid Earth to past and present changes in surface AIS load. The vertical deformation rates derived from GPS measurements represent the integrated signal of several processes operating on various timescales. The two primary contributing factors to vertical land motion are the remaining slow viscous response to past ice and water load changes and the near-instantaneous elastic response due to contemporary ice load changes (Martín-Español et al., 2016; Sasgen et al., 2017).

GPS observations have previously been implemented to evaluate Antarctic GIA and ice sheet models (Argus et al., 2014; Gomez et al., 2018; Whitehouse et al., 2012b; Ivins et al., 2013). The resulting Antarctic GIA estimates are used in conjunction with satellite-derived remote gravimetry or altimetry data to infer contemporary mass balance changes of the AIS (Shepherd et al., 2018).
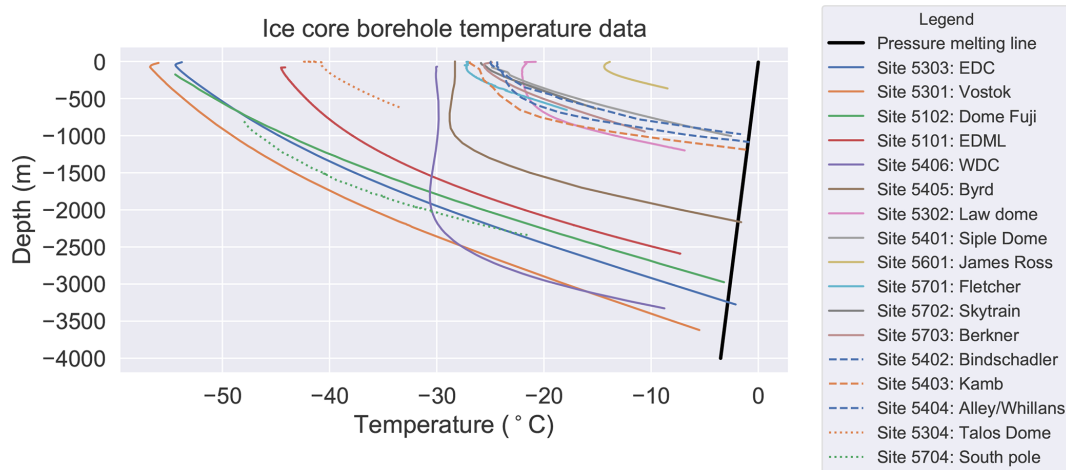
Figure 6. Ice core borehole temperature (boreTemp) data to illustrate the data quality and tier assignment. The dashed lines represent the sites in the Siple Coast which are tier-2 data, and the dotted lines represent the most limited borehole temperature data which do not cover the majority of the ice column (tier-3 data).

GPS deformation rates first have to be corrected for the elastic response to contemporary ice mass change before they can be inferred to reflect the background viscous response to past ice mass change (Martín-Español et al., 2016; Sasgen et al., 2017). For our database, a key criterion for GPS data evaluation is the constraint value for Antarctic GIA. We therefore divide the dataset into stations that are not influenced significantly by modern ice mass change and stations with a significant contemporary elastic signal (for details, see the discussion section below). A total of 67 GPS stations constrain the isostatic adjustment of the land bedrock for the period 2009 to 2014, with a total of 15 GPS stations being assigned to a high-quality tier (as discussed in Sect. 3.1.5).

Alongside the GPS uplift rates, we provide the elastic-response-corrected vertical rates from Martín-Español et al. (2016). Both the GPS and elastic-corrected datasets come associated with their own explicit and implicit uncertainties. In compiling the AntICE2 GPS dataset, we selected sites that are hardly impacted by contemporary mass balance changes (negligible elastic signal). The accuracy of the elastic-corrected high-quality subset of GPS data is dependent on the validity of the inferred contemporary ice load changes and the resulting elastic signal.

2.6 Present-day geometry and surface ice velocity

The AIS geometry from BedMachine Antarctica version 2 provides the primary PD constraint and initialization conditions (BCs) (Morlighem et al., 2020). This directly constrains several key PD metrics by comparing the modelled ice sheet to contemporary observations, namely ice thickness mean-squared errors (MSEs) for East Antarctica, West Antarctica, and all ice shelves; squared errors of latitudinal and longitudinal grounding-line positions along five key tran-

sects shown in Fig. 2a (Ross, Amundsen, Ronne, Filchner, and Amery transects); squared errors of grounded and total ice area; squared errors for the ice shelf area across five sectors (Ross, Amundsen–Bellingshausen, Weddell, Lambert–Amery, and all other remaining sectors combined). These PD observations provide powerful spatial constraints but limited temporal constraints that only extend back into the late Holocene. The grounding-line transects and sector margins are shown in Fig. 2a. The specific locations of these metrics, particularly the transects, were chosen to investigate areas sensitive to past and present ice sheet changes. The data provided by BedMachine have a horizontal resolution of 500 m by 500 m and include 2σ uncertainties on ice thickness inferences (Fig. 7a–d). The topographic fields must be upscaled to the appropriate resolution for a given ice sheet model grid; the metrics discussed above are then calculated at this resolution for consistency. As part of the NASA-funded Making Earth System Data Records for Use in Research Environments (MEaSUREs) programme, surface velocities of the AIS have been made available for the period from 2005 to 2017 (Mouginot et al., 2019) (Fig. 7e–f). The surface velocity dataset is remotely derived from satellite data provided at a horizontal resolution of 450 m by 450 m, which is similarly upscaled to the ice sheet model grid resolution for data–model comparison and inversion.

2.7 Data uncertainty structure

The uncertainties in the database are explicitly stated as 1σ and 2σ intervals. Some of the observational data in the database exhibit two-way or one-way bounds. It follows that some proxy data and their uncertainties represent just an upper- or lower-bound constraint (one-way bounds). Two-way Gaussian uncertainties are affiliated with the PD obser-
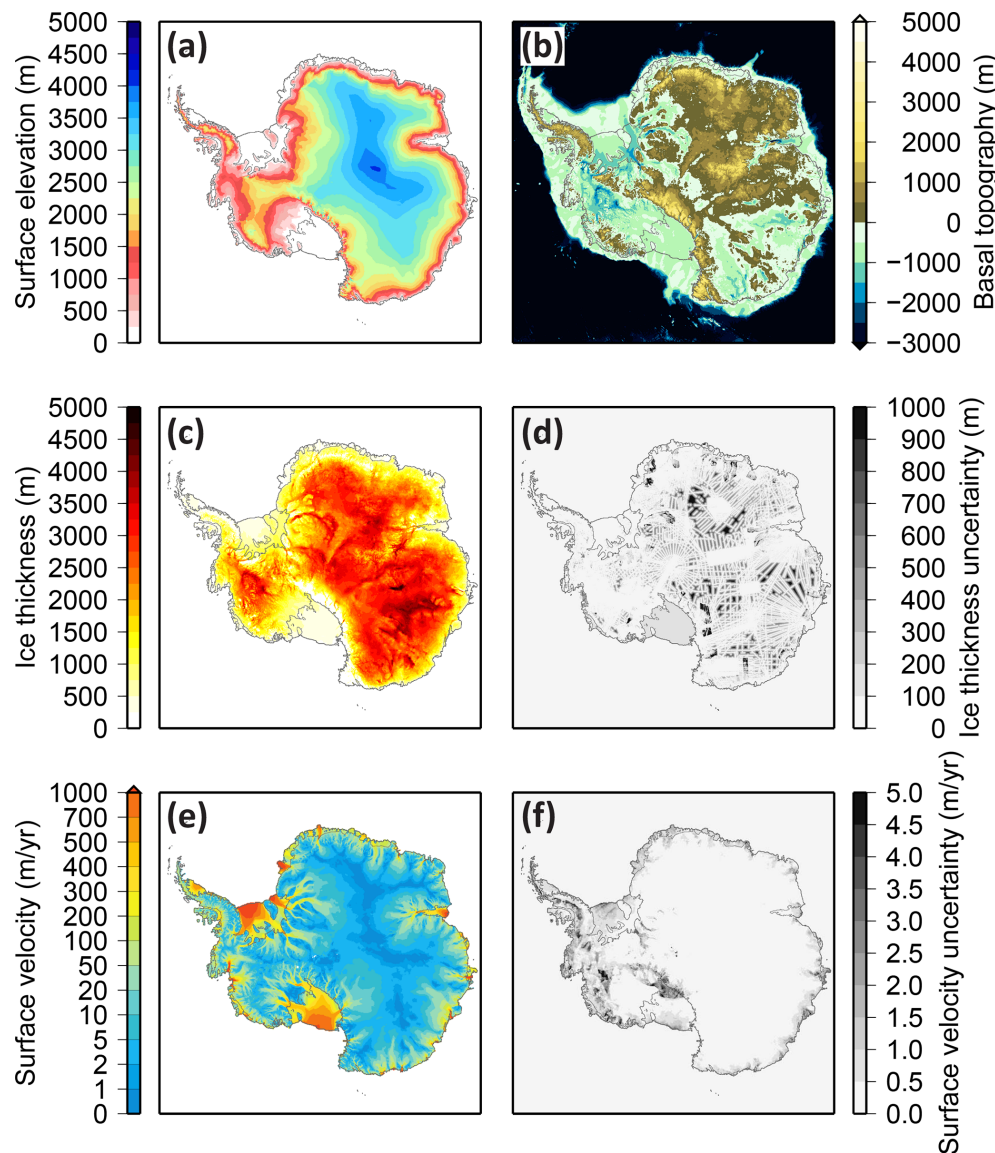
Figure 7. (a–d) Present-day Antarctic Ice Sheet geometry based on the BedMachine version 2 PD data (Morlighem et al., 2020) and **(e–f)** MEaSUREs ice surface velocity over 2005–2017 and its associated uncertainties (Mouginot et al., 2019).

vations (ice sheet geometry and surface velocities), the GPS observations, and borehole temperature measurements. The paleoH and paleoExt data are also represented by two-way symmetric uncertainties around the mean. Some of the paleoExt data constrain exclusively the onset of open-marine conditions, rendering them a one-way constraint. There are several one-way constraints in the RSL database as well, such as those that are limiting minimum or maximum RSL inferences (molluscs, penguin remains). The details are specified in the database itself and were previously discussed in greater detail in Briggs and Tarasov (2013). These observations are converted to nominal two-way non-symmetric constraints by assigning an exceedingly small or large uncertainty bound to the unspecified region of the probability distribution. This

adoption of a Gaussian observational error model facilitates ice history scoring. However, the validity of a Gaussian error model for all the types of data in our database awaits future testing.

3 Discussion

The implementation of a database for geophysical model calibration has a number of requirements to ensure utility. In large part this boils down to clear specification of the relationship between the data and the real-world system under consideration. As such, the database curation process and all data uncertainties need to be clearly specified. From the perspective of modellers, a careful evaluation of internal and ex-
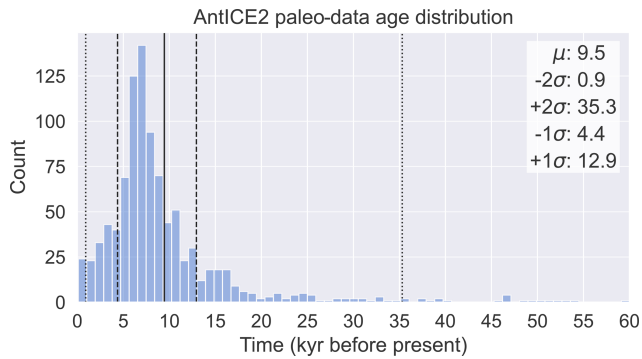
Figure 8. Age distribution of AntICE2 paleo-data (paleoExt, paleoH, paleoRSL), with the vertical solid line, dashed lines, and dotted lines representing the mean, $\pm 1\sigma$, and $\pm 2\sigma$ ranges, respectively. The 1σ and 2σ bounds correspond to the nominal 68 % and 95 % confidence intervals. The skewed distribution has a median value of 7.4 ka.

ternal model limitations is necessary to produce meaningful data–model comparisons. In this discussion, some considerations are explicitly stated when it comes to the aforementioned challenges.

For much of the last glacial cycle, there are very few to no paleo-observations that directly constrain the configuration of the ice sheet (Fig. 8). The paleo-data (paleoEXT, paleoH, paleoRSL) have a mean age of 9.5 ka and a non-uniform distribution with a long tail of older ages beyond the LGM. A total of 81 % of the paleo-data have a Holocene age (< 11.7 ka). However, some data points integrate ice sheet behaviour over a period and so have constraining power far exceeding their measured age (e.g. PD borehole temperature data – Ackert, 2003).

The heterogeneity in the spatial distribution of the data is illustrated in Fig. 2. Data of a given type constrain the surrounding region based on the data type and data quality. This is due to the spatial correlation of certain ice sheet system changes such as margin retreat or GIA. For instance, past ice thickness data might constrain localized ice elevation changes for a particular glacier only. In contrast, past RSL data document changes in the bedrock and geoid elevation, which is a spatially smooth signal. Each data point has a specific spatio-temporal sphere of influence, which defines its ability to constrain the model. Figures 2 and 8 illustrate areas in space and time with clear data gaps and densely sampled areas. Thus, this heterogeneity highlights the importance of never equally weighing all the data when scoring since it would introduce major biases in an ice sheet model calibration. An inverse-areal weighing of the data can be used to avoid overfitting the model to a particular region with high data density if the correlation between data–model residuals is not otherwise accounted for (Tarasov and Goldstein, 2021).

Field observations are often collected in Antarctic regions with a complex and highly variable topography that is inadequately resolved in typical Antarctic-wide ice sheet simulations. Thus, the more a datum embodies broader characteristics of the glacial system as opposed to reflecting subgrid characteristics, the higher its potential constraint value. For data containing a significant subgrid signal, some combination of upscaling of the data and/or downscaling (potentially including subgrid modelling) of the model results will be required but may not always be physically justifiable. The RSL change, borehole temperatures, and GPS rates represent spatially and temporally smooth proxies and require no upscaling corrections. The marine paleoExt data capture rather broad nonlinear changes in the GL, sub-ice-shelf, or open-marine characteristics. However, for GL sites near the continental shelf break, the gridded topography could potentially designate areas at the shelf break as immediately off the continental shelf, for which the model would never produce grounded ice. Some terrestrial data, such as nunatak indicators, may also predominantly reflect subgrid high-frequency features that will therefore not be resolved by the model. Given fundamental model limitations, such as grid resolution, for most if not all data, the physical signal represented by the data (i.e. after accounting for observational uncertainties) will only be incompletely resolvable by the model even after appropriate upscaling and/or downscaling. The resultant fundamentally irreducible discrepancy between the model results and geophysical system will then need to be accounted for in the error model describing the relationship between the model and physical system (see Sect. 3.1.8).

The uncertainties associated with the indicative meaning of various proxy data must be considered when estimating observational uncertainties. This is particularly relevant for the paleoExt data because ocean currents can advect particles from open water beneath an ice shelf so that the resulting deposits resemble open-marine facies. This can be up to 6 and 100 km from the calving front for small and large ice shelves, respectively (Riddle et al., 2007; Post et al., 2014; Hemer and Harris, 2003; Hemer et al., 2007). Similarly, facies characterizing sediments deposited proximal to the GL (PGL) can form up to 10 km seaward from the GL at the time of formation (Smith et al., 2019). When it comes to paleoRSL data, considerations should be made for the fact that storm surges can impact the in situ deposition of certain proxy data. This has previously been handled by applying a storm beach adjustment factor of up to 1 m for proxy data from, but not limited to, mollusc fragments and penguin bones (Briggs and Tarasov, 2013). This information is not integrated within the AntICE2 database, and we defer with regard to the incorporation of such uncertainties within a data–model-scoring implementation.

3.1 Data curation and tiered data quality assessment

To facilitate data–model comparison, the paleo ice extent, ice thickness, relative sea level, borehole temperatures, and PD uplift rates are all curated, and individual data points are categorized into quality tiers (Table 1). Tier 1 is the highest quality tier, while tier 3 is the lowest accepted tier (for example, see Fig. 3). Tier-1 data have the greatest power to constrain the ice sheet and GIA history. For example, in the case of cosmogenic-exposure dating, key exposure ages capturing both the LGM ice thickness and timing of deglaciation prove to be most valuable since they constrain the most prominent deglacial changes. Tier-2 data typically represent data with less constraining power that primarily supplement tier-1 data. Returning to the previous exposure data example, tier-1 data represent a minimal set of crucial tie points for the LGM ice thickness and timing of deglaciation, while tier-2 data provide finer detail for the deglacial ice-sheet-thinning history, with minimal correlation to other data. Finally, tier-3 data include lower-quality observations that exhibit a high degree of correlation with tier-1 and tier-2 data and for which data uncertainty specifications are less confident. The tier assignment depends on data type, data availability, and data density. This particularly becomes an issue at sites with limited observations. When mentioning lower-quality data, we refer to data with larger measurement or analytical uncertainties or limitations due to a proxy's indicative strength (i.e. whether its interpretation is ambiguous or not). Data that are not assigned to a quality tier typically represent redundant data, data with very large uncertainties, data which do not accurately represent the local environmental history, or where original publications note potential analytical problems. In the case of cosmogenic-nuclide data, exposure ages that clearly suffer from inheritance are not assigned to a quality tier. Moreover, some data are excluded from tier assignment based on physical impossibility – e.g. exposure age data require that younger ages must be at a lower elevation than older ages for a given site. In the following subsections, we describe the tier assignment process which involves evaluating the datasets with respect to strict criteria that assign the datasets to their respective tiers. Further refinements are conducted based on expert assessment and outlier identification. This is performed on a data type basis with the aim of minimizing subjectivity in quality assessment and data selection. There are a few criteria which are consistent across data types: prioritizing data with a high signal-to-noise ratio beyond a chosen data type threshold; valuing data in data-sparse regions; outlier identification and exclusion when substantiated by broadly consistent, dense data clusters (cluster density assessments are data type dependent); and superfluous data exclusion. Some data are assigned to a tier of -1, which signifies that the observation should be entirely excluded for data–model comparison since it failed one or several quality criteria. This tier equal to -1 is solely for the

Table 1. Summary of Antarctic Ice Sheet Evolution database version 2 (AntICE2) and quality tier subsets.

Data type	All data	Tier-1 data	Tier-2 data	Tier-3 data
Past ice extent (paleoExt)	249	63	15	30
Past ice thickness (paleoH)	2710	108	348	270
Past relative sea level (paleoRSL)	425	23	48	52
Ice core borehole temperature (boreTemp)	36 740	36	9	6
Present-day GPS uplift rates (rdotGPS)	67	6	9	–
AntICE2	40 191	236	429	358

purpose of logging the data and identifying it as not trustworthy to ensure exclusion from analyses.

3.1.1 PaleoH data curation

The past ice thickness dataset requires additional considerations when assessing data tiers. Some paleoH sites have few exposure ages that constrain the elevation history. In these instances, we rely on the discretion of the original study to assess the quality of the data point which is available through ICE-D. At a given site, an assessment is conducted that identifies the highest-quality exposure ages (e.g. ^{10}Be, ^{26}Al, ^{3}He, and ^{14}C) bracketing the elevation history and sorts the data into tiers (Figs. S1–S102 in the Supplement). A high data density cluster of young exposure ages that form the expert-assessed 2σ bounds on elevation history is identified (Fig. 3). This assessment considers the occurrence of inheritance and post-deglacial shielding. By evaluating paired isotope exposure ages and applying first principles (along a sample transect, older ages should always be obtained from samples collected at higher altitudes), many data points can be excluded, and an expert-assessed 2σ elevation history based on data density can be identified. Tier-1 data are the data constraining the magnitude, timing, and rate of elevation change over the deglaciation. Tier-2 data further constrain the specific structure of the elevation history. Tier-3 data include the remaining pertinent data, which fully populate much of the expert-assessed 2σ bounds on elevation history. The primary reason for tier-3 data to be relegated to their own tier rather than being included in the tier-2 data is the limited constraining power that they introduce to past ice thickness changes given how they correlate significantly with tier-1 and tier-2 data, which renders them nearly superfluous in many instances. When evaluating a cluster of neighbouring sites, a certain degree of consistency should be expected if the expo-

sure data are truly representative of a broader region rather than extremely local ice elevation changes. Therefore, an additional iteration on the tiers is performed based on upstream or downstream consistency with neighbouring paleoH sites to identify potential outliers. The source literature of Antarctic exposure ages does not always report the sample position relative to the mean flow of the surrounding ice. This proves to be an issue when comparing ice-thinning histories reconstructed by continental-scale ice sheet models with histories based on paleoH data because the exposure ages can be heavily biased depending on the nunatak flank, where the samples were collected (Mas E Braga et al., 2021). This information is not broadly accessible in the source literature, causing a limitation which propagates into the AntICE2 database, and this must be considered within the error model when scoring a reconstruction against paleoH data.

3.1.2 PaleoExt data curation

The past-ice-extent dataset is also divided into tiers based on specific data type criteria. Firstly, the interpretation of the facies is extracted from the source literature and assigned one of the following classes (Figs. 4 and S103–S180 in the Supplement): proximal to the GL (PGL), sub-ice-shelf (SIS), or open-marine conditions (OMC). Each core is then sorted according to the ^{14}C dating method, i.e. whether the ^{14}C age is obtained from biogenic carbonate or organic matter, with the latter dates typically considered to be less reliable (see Sect. 2.2). Down-core ^{14}C ages obtained from organic matter in sediment cores from the Antarctic continental shelf are often corrected by subtracting the core top age rather than the marine reservoir effect only (e.g. Domack et al., 1999; Pudsey et al., 2006). This approach assumes that the degree of contamination of young organic carbon with reworked fossil organic matter has remained constant throughout the record; however, this is often not the case (e.g. Heroy and Anderson, 2007). For these reasons, ^{14}C ages on calcareous microfossils, if present, are typically favoured over organic matter ^{14}C ages, and the former are typically assigned to a high-quality tier. Additional criteria for sorting the paleoExt data into tiers are based on the overall quality of the marine sedimentary record and facies interpretation, specifically whether the stratigraphy of the core is affected by reworking (e.g. due to iceberg turbation). Moreover, if in a given core multiple dates were obtained from different facies that indicate the same environmental conditions, the maximum and minimum dates bracketing the age cluster are assigned to a high-quality tier, whereas the remaining dates are excluded to avoid redundancy. These criteria are enforced when assigning tiers to the marine paleoExt data and when deciding whether to exclude ages from direct data–model scoring.

3.1.3 PaleoRSL data curation

Compared to other data types, there are limited past RSL observations. For this reason, the quality assessment of the paleoRSL data is performed on a site-by-site basis. For a given site, we define the expert-assessed 2σ bounds on RSL history as being constrained by sea level index points and minimum and maximum bounds (Figs. 5 and S181–S192 in the Supplement). This approach inherently identifies potential outlier data for exclusion. Tier-1 data for a site comprise the highest-quality proxy data that constrain the highstand and the form of the deglacial sea level fall. Data that constrain the RSL history with minimal redundancy and supplement tier-1 data are assigned to a tier-2 status. The classification of tier-2 data is based on data density along the expert-assessed 2σ bounds on theoretical RSL history (Fig. 5). Tier-3 RSL data further populate the most likely RSL history already defined by the tier-1 and tier-2 data and provide lower-quality constraints that correlate to tier-1 tier-2 data without being completely superfluous.

3.1.4 Borehole temperature data curation

The ice-core borehole temperature profiles consist of a significant amount of data along a single profile, much of which is highly correlated with depth. Therefore, a subset of the profile data is chosen and assigned to a tier-1 quality for data–model scoring. The tier-1 data consist of the coolest near-surface ice temperature, the nearest basal ice temperature, and the ice column midpoint englacial temperature. These data alone can effectively constrain the structure of the simulated temperature profile given the smoothness of the signal. South Pole and Talos Dome borehole temperature profiles were the only profiles that did not cover the majority of the ice column (Fig. 6). Therefore, they provide less constraining power on a model and are assigned a tier-3 status. The Siple Coast borehole profiles from the Siple Dome, Bindschadler, Kamb, and Alley–Whillans ice streams are relatively proximal and correlate with each other, so they are assigned a tier-2 status except for the Siple Dome profile which remains the regional tier-1 representative. The other ice core borehole temperature profiles (solid-coloured lines in Fig. 6) are all part of the tier-1 subset because of the quality and location of the data (Fig. 2d). Each respective borehole temperature profile is reduced to three data points (surface, englacial, and basal ice temperature) that most meaningfully represent the entire profile (Table 1).

3.1.5 Uplift rate data curation

PD uplift rates inferred from GPS observations constrain several integrated processes. Prior to sorting the GPS uplift rates into tiers, the GPS data must be evaluated to identify a subset which is most suitable to constraining the GIA signal and hence past ice load changes. First and foremost, contemporary ice sheet change triggers an elastic response that

contributes to the PD observed uplift rates and hence masks the signal associated with past ice sheet change. GPS data from sites where significant PD elastic contributions were inferred (Fig. S193 in the Supplement) are considered to be low-quality constraints on the contemporary GIA signal and hence on the past ice load changes. Several criteria, such as a low elastic correction ($< 0.55\,\mathrm{mm\,yr^{-1}}$) and a small uplift rate standard deviation ($< 1\,\mathrm{mm\,yr^{-1}}$) or high signal-to-noise ratio (> 1.45), determine which GPS data are considered for data–model evaluation and tier classification. Additionally, GPS sites that are in the vicinity of the coast ($< 250\,\mathrm{km}$) or in areas where significant mass loss has evidently occurred over the last millennium are excluded from being classified into a tier. The GPS data that pass these criteria are assigned a preliminary tier-2 status. A final criterion considers a common model limitation, which pertains to the spherically symmetric viscosity profile of many GIA models and excludes the presence of lateral viscosity structure. This criterion can be disregarded if dealing with a 3D Earth viscosity model. In several regions of West Antarctica, the continental crust is underlain by a mantle with anomalously low viscosities in the top $250\,\mathrm{km}$ (Whitehouse et al., 2019). GPS sites near anomalous viscosity features are more capable than others of biassing the model calibration given the structural uncertainty associated with the GIA model. Therefore, certain sites are identified along parts of the Antarctic Peninsula and in the Amundsen–Bellingshausen Sea sector and the Ross Sea sector, where the inferred viscosity at depth is below $10^{20}\,\mathrm{Pa\,s}$ (Whitehouse et al., 2019). These criteria filter the GPS uplift rate data based on their quality and ability to constrain the GIA signal and past ice load changes. One persisting issue is the robustness of the elastic corrections, which are likely to have underrepresented uncertainties (Martín-Español et al., 2016). Uncertainties in the elastic corrections can be increased by the root sum square, with the elastic correction boosting confidence that the elastic-corrected uplift rates accurately constrain the viscous GIA response. Of the tier-2 GPS sites, those which are not located in regions with anomalously low mantle viscosity are promoted to tier-1 quality status (six sites). The exact thresholds for the various criteria are based on the need to identify a higher-quality data subset while simultaneously accounting for unquantified uncertainties associated with the elastic corrections. The criteria-defined higher-quality subset size is chosen to represent the top third of tiered GPS data (tier-1 and tier-2 data), offering sites that are especially sparsely distributed. Refinements to the criteria thresholds will be required as the size of the GPS network evolves and as more robust approaches to interpreting GPS time series are developed.

3.1.6 Present-day AIS geometry data curation

The PD AIS geometry and surface velocities are crucial constraints that provide nearly complete spatial coverage, ren-

dering them tier-1 data. Regions with large uncertainties in the PD AIS bed geometry and surface velocities could be classified as tier-2 data points; however, given that these regions typically have no other data constraints, they remain top-tier data. For scoring ice sheet model simulations against them, it is important to account for the uncertainties in these inferences when calculating a root-mean-square-error score. It has been shown that spectral noise models, which introduce spatially correlated noise, can be used to produce an ensemble of boundary conditions that are self-consistent with the underlying field and uncertainty estimates (Sun et al., 2014; Gasson et al., 2015). This provides a method that allows for a proper quantification of uncertainties affiliated with these boundary conditions.

3.1.7 Data standards and expert assessment

Fundamental and recurring issues, which exacerbate the challenges of evaluating data quality, remain across many studies and data types. They relate to the data availability. For example, some studies make the entirety of uncorrected, corrected, and calibrated ^{14}C ages available (Heroy and Anderson, 2007; Bentley et al., 2014b), while others provide only those with robust interpretations. This makes it challenging to assess the entirety of a broad dataset by the same standards since some data rely on the implicit assessments made by their respective study. Ideally, all associated data should be made available, and the data should be categorized into quality tiers based on explicitly specified criteria. The expert quality control by the principal investigators who collected the samples and analysed and evaluated the data is exceedingly valuable and should be included with the data. This enables a broader consensus on quality control as various experts converge towards specific quality criteria. Moreover, when new proxy data of various qualities are introduced in the future, including potential novel constraints, it will be possible to re-assess the categorical quality tiers if their criteria are clearly specified. The data made available should contain all the necessary information to recalibrate the data with clearly specified uncertainties. This will facilitate future data calibration, standardization, and quality assessment once integrated properly within an online repository, such as the ICE-D repository (Balco, 2020).

3.1.8 Data–system and system–model uncertainties

The data presented in the AntICE2 database include data–system uncertainty, typically referred to as observational uncertainty, which consists of measurement uncertainty and indicative meaning uncertainty. The former represents uncertainties affiliated with inherent instrumental uncertainties when taking measurements, such as the elevation at which a sample for exposure dating is collected. The latter represent uncertainties relating to the interpretation of data and how these data represent a proxy observation for physical

characteristics of the system, for instance a fossil mollusc fragment and how it relates to past sea level. In the AntICE2 database, we include the indicative meaning uncertainty from the source literature when available and otherwise do not attempt to specify it. On the other hand, we do specify a baseline measurement uncertainty when this is absent in the source publication or when it is clearly understated.

As the observational uncertainty specifies the data–system relationship, meaningful data–model comparison also requires specification of the relationship between the model and the physical system. However, appropriate specification of the structural error model is a major challenge. The source of this challenge is that we cannot have complete knowledge of the current and especially of the past state of the Earth system or any significant sub-component thereof. As such, we cannot easily identify and quantify model deficiencies with respect to the system of interest. There are many approaches for dealing with these challenges, and we point the reader to Tarasov and Goldstein (2021) for a broader discussion.

3.2   Potential future and rejected data types

Radiostratigraphy of the Greenland Ice Sheet has been used to infer the age structure of the ice sheet (MacGregor et al., 2015). Proof-of-concept age-tracking simulations of a 3D slice through the Greenland summit have demonstrated the potential constraint value of such data (Born, 2017). The age structure of the ice is inferred from internal radar reflectors (reflective isochrones) visible in the radiostratigraphic profiles, which are dated at major ice core sites (Cavitte et al., 2021). The AntICE2 database does not include any direct age structure constraints for the Antarctic Ice Sheet. It would be extremely valuable to have an age structure for the entire AIS because this would provide constraints for many regions that are lacking any paleo-constraints. However, the presently available radiostratigraphy coverage for the AIS is spatially limited, and as such, no such AIS-wide reconstruction currently exists. The depth–age data from ice cores can directly constrain the age structure. Moreover, there are some regional age reconstructions for well-studied regions and transects (Ashmore et al., 2020; Winter et al., 2019; Delf et al., 2020; Cavitte et al., 2021). A compilation of age reconstructions has been started under the AntArchitecture initiative within the Scientific Committee on Antarctic Research (SCAR) (https://www.scar.org/science/antarchitecture/antarch-news/, last access: 6 July 2023). Sutter et al. (2021) demonstrate a data–model comparison of various age isochrones in Antarctica and illustrate the utility of this new data type. As accurate ice-age-tracing modules become available for ice sheet models, radiostratigraphic age constraints will provide a powerful new constraint on past AIS evolution.

Ice cores have previously been used to infer past AIS elevation changes relative to PD. Originally this was done by analysing the gas content trapped in the ice (Lorius et al.,

1984; Delmotte et al., 1999), relating the total gas content to the ambient atmospheric pressure at bubble close-off. This traditional method produces a high noise-to-signal ratio, especially because other processes affect the volume of open pore space in the ice, such as insolation (Raynaud et al., 2007) and climate (Eicher et al., 2016). We therefore do not include air content observations in the AntICE2 database. An alternative method to determine past elevation changes at ice core sites is through model inferences, where model simulations are locally constrained by ice core data (Barbante et al., 2006; Neumann et al., 2008; Steig et al., 2001; Waddington et al., 2005; Parrenin et al., 2007). The issue with using model inferences to constrain a model is that they integrate all the assumptions involved in making those inferences, and these are often not explicitly specified. Moreover, the uncertainties in the ice core site elevation model inferences are often inadequately explored and hence underestimated and would benefit from a greater exploration of the range of uncertainties (Steig et al., 2001). If included in a calibration, this would propagate ill-defined uncertainties and could invalidate the calibration. Therefore, we opt to exclude this dataset since it is too far removed from direct field observations and comes associated with significant and ill-defined model uncertainties.

As previously mentioned when discussing the GPS data, geodetic observations have been used to constrain the GIA response signal associated with past ice sheet changes (Martín-Español et al., 2016; Sasgen et al., 2017). The justification for excluding the inversion-based Antarctic GIA reconstructions as a constraint lies in the assumptions behind the elastic corrections associated with contemporary mass loss. Like the ice-core-inferred elevation changes, the elastic corrections come associated with ill-defined model uncertainties which could invalidate the calibration if implemented without expanded uncertainties. Moreover, if the intention is to calibrate an ice sheet and GIA model to infer contemporary mass balance by correcting geodetic data, it would be circular reasoning to apply a constraint that makes a priori assumptions about the form of the GIA signal.

Several ice cores have been drilled to the bed across the Siple Coast, and the retrieved basal till frequently contains organic material yielding ^{14}C ages significantly younger than 40 ka but older than 20 ka (Kingslake et al., 2018). This poses the question of whether the GL retreated landward from the core sites during the most recent deglaciation. The presence of organic matter with a last-glacial-period age at the base of the modern AIS is hard to reconcile because all major continental ice sheets, including the AIS, are believed to have reached their maximum extent and size during this time. Subglacial sediments contain mixtures of eroded and reworked detritus initially deposited at different times. Therefore, a ^{14}C date obtained from the organic matter of such subglacial sediments typically provides an integrated age, derived from the mixing of relatively young with old and even ^{14}C-dead material, which increases the uncertainty of how to interpret such

a date. Kingslake et al. (2018) opted to use the ^{14}C dates as evidence of an early Holocene GL retreat upstream of its PD position, thereby arguing that the ^{14}C dates do not represent true ages for sediment deposition ages. Given these uncertainties and notwithstanding further studies (Neuhaus et al., 2021) on the ^{14}C dates from the till samples along the Siple Coast, these observations have not been included in the AntICE2 database as paleoExt GL retreat constraints because they do not yet represent a firm and reliable age constraint on GL position.

The main outstanding issues with the AntICE2 database are the temporal and spatial data gaps. As shown in Figs. 1, 2, and 8, only a small number of dates extend beyond 20 ka, and the spatial distribution of the data leaves many regions, particularly in East Antarctica, completely devoid of observational constraints. The ramification of the data deserts is that calibrated models will likely have large uncertainties in regions with limited observational constraints. A few new data types, discussed above, could ameliorate the situation, with the most promising being the wide-scale age structure of the AIS, inferred from airborne and on-ice radar mapping of internal layering connected to sites of dated ice cores. This data type could constrain changes in the AIS far beyond 30 ka and even cover regions with little or no data due to a lack of rock outcrops and boreholes.

Future work should focus on using calibrated model results to establish an Antarctic treasure map, similar to that produced for ice cores by Bradley et al. (2012), which identifies high-priority targets for the collection of observational data (Tarasov and Goldstein, 2021). Such a map would highlight the constraining power of various hypothetical observational constraints, for example, those taken from unsampled nunataks or paleo-grounding-zone wedges preserved on the continental shelf. Finally, this future progress crucially depends on the growth of well-maintained online data repositories (e.g. ICE-D, Ghub), the careful curation of data, the standardization of the curation criteria, and the proper methodological approaches toward data–model comparison.

4 Data availability

The Supplement contains plots of the entire tiered AntICE2 database. Summary plots provide concise representations of various data types when possible. The AntICE2 database can be downloaded as Excel tables (.xlsx) from the Supplement, and the latest version is in the online repository https://theghub.org/resources/4884 (Lecavalier et al., 2022).

5 Summary

In this study, we provide the second major iteration of the Antarctic Ice Sheet Evolution observational constraint (AntICE2) database. The AntICE2 database is a curated observational constraint database intended for the calibration of models of the Antarctic Ice Sheet and Antarctic glacial isostatic adjustment over the last glacial cycle. It can also be used to constrain a paleo-model spin up of the AIS to initialize PD simulations. This will lead to a more accurate understanding of contemporary and future changes of the AIS. The AntICE2 database includes a large variety of observational constraints necessary for model calibration. The data types included are as follows: PD geometry and surface velocity, PD uplift rates, borehole temperature profiles, past ice extent, past ice surface elevation, and past relative sea level. All the ^{14}C ages in the database are recalibrated and share a consistent reservoir age correction wherever appropriate. The AntICE2 database represents a curated dataset with specified quality tiers. This was achieved by establishing and applying criteria for the different data types. Future efforts should be geared toward refining the criteria for the quality tier assignment since a community consensus would benefit data–model integration. An ongoing effort involves automating the selection and curation process from a raw database (ICE-D) to a recalibrated curated subset (i.e. AntICE2). This would render the AntICE2 database more manageable and updatable when more data are being collected in the future. To contribute to the AntICE2 database, one can contact the corresponding author with data or publications, contribute data to the ICE-D databases, or offer data type criteria modifications to help revise the data curation process. The AntICE2 database represents the most comprehensive observational constraint dataset of high-quality data relating to the past evolution of the Antarctic Ice Sheet. The dataset facilitates data integration with AIS and GIA simulations. This dataset compilation also facilitates data–model scoring by processing and curating large raw and disparate datasets from online repositories (e.g. ICE-D) and source publications. Finally, a call to the community is made to make raw data with complete and clearly specified uncertainties publicly available and to make efforts towards establishing data quality criteria in order to facilitate data curation and hence produce meaningful data–model comparisons.

References

Ackert, R. P.: An ice sheet remembers, Science, 299, 57–58, https://doi.org/10.1126/science.1079568, 2003.

Ackert, R. P., Barclay, D. J., Borns, H. W., Calkin, P. E., Kurz, M. D., Fastook, J. L., and Steig, E. J.: Measurements of Past Ice Sheet Elevations in Interior West Antarctica, Science, 286, 276–280, https://doi.org/10.1126/science.286.5438.276, 1999.

Ackert, R. P., Mukhopadhyay, S., Parizek, B. R., and Borns, H. W.: Ice elevation near the West Antarctic Ice Sheet divide during the Last Glaciation, Geophys. Res. Lett., 34, 1–6, https://doi.org/10.1029/2007GL031412, 2007.

Albrecht, T., Winkelmann, R., and Levermann, A.: Glacial-cycle simulations of the Antarctic Ice Sheet with the Parallel Ice Sheet Model (PISM) – Part 1: Boundary conditions and climatic forcing, The Cryosphere, 14, 599–632, https://doi.org/10.5194/tc-14-599-2020, 2020.

Anderson, J. B., Conway, H., Bart, P. J., Witus, A. E., Greenwood, S. L., McKay, R. M., Hall, B. L., Ackert, R. P., Licht, K., Jakobsson, M., and Stone, J. O.: Ross Sea paleo-ice sheet drainage and deglacial history during and since the LGM, Quaternary Sci. Rev., 100, 31–54, https://doi.org/10.1016/j.quascirev.2013.08.020, 2014.

Argus, D. F., Peltier, W. R., Drummond, R., and Moore, A. W.: The Antarctica component of postglacial rebound model ICE-6G_C (VM5a) based on GPS positioning, exposure age dating of ice thicknesses, and relative sea level histories, Geophys. J. Int., 198, 537–563, https://doi.org/10.1093/gji/ggu140, 2014.

Arndt, J. E., Hillenbrand, C. D., Grobe, H., Kuhn, G., and Wacker, L.: Evidence for a dynamic grounding line in outer Filchner Trough, Antarctica, until the early Holocene, Geology, 45, 1035–1038, https://doi.org/10.1130/G39398.1, 2017.

Arndt, J. E., Larter, R. D., Hillenbrand, C.-D., Sørli, S. H., Forwick, M., Smith, J. A., and Wacker, L.: Past ice sheet–seabed interactions in the northeastern Weddell Sea embayment, Antarctica, The Cryosphere, 14, 2115–2135, https://doi.org/10.5194/tc-14-2115-2020, 2020.

Ashmore, D. W., Bingham, R. G., Ross, N., Siegert, M. J., Jordan, T. A., and Mair, D. W. F.: Englacial Architecture and Age-Depth Constraints Across the West Antarctic Ice Sheet, Geophys. Res. Lett., 47, e2019GL086663, https://doi.org/10.1029/2019GL086663, 2020.

Balco, G.: Technical note: A prototype transparent-middle-layer data management and analysis infrastructure for cosmogenic-nuclide exposure dating, Geochronology, 2, 169–175, https://doi.org/10.5194/gchron-2-169-2020, 2020.

Balco, G. and Schaefer, J. M.: Exposure-age record of Holocene ice sheet and ice shelf change in the northeast Antarctic Peninsula, Quaternary Sci. Rev., 59, 101–111, https://doi.org/10.1016/j.quascirev.2012.10.022, 2013.

Balco, G., Stone, J. O., Lifton, N. A., and Dunai, T. J.: A complete and easily accessible means of calculating surface exposure ages or erosion rates from ^{10}Be and ^{26}Al measurements, Quat. Geochronol., 3, 174–195, https://doi.org/10.1016/j.quageo.2007.12.001, 2008.

Balco, G., Todd, C., Huybers, K., Campbell, S., Vermeulen, M., Hegland, M., Goehring, B. M., and Hillebrand, T. R.: Cosmogenic-nuclide exposure ages from the Pensacola Mountains adjacent to the foundation ice stream, Antarctica, Am. J. Sci., 316, 542–577, https://doi.org/10.2475/06.2016.02, 2016.

Balco, G., Todd, C., Goehring, B. M., Moening-Swanson, I., and Nichols, K.: Glacial geology and cosmogenic-nuclide exposure ages from the Tucker glacier – Whitehall glacier confluence, northern Victoria Land, Antarctica, Am. J. Sci., 319, 255–286, https://doi.org/10.2475/04.2019.01, 2019.

Barbante, C., Barnola, J. M., Becagli, S., Beer, J., Bigler, M., Boutron, C., Blunier, T., Castellano, E., Cattani, O., Chappellaz, J., Dahl-Jensen, D., Debret, M., Delmonte, B., Dick, D., Falourd, S., Faria, S., Federer, U., Fischer, H., Freitag, J., Frenzel, A., Fritzsche, D., Fundel, F., Gabrielli, P., Gaspari, V., Gersonde, R., Graf, W., Grigoriev, D., Hamann, I., Hansson, M., Hoffmann, G., Hutterli, M. A., Huybrechts, P., Isaksson, E., Johnsen, S., Jouzel, J., Kaczmarska, M., Karlin, T., Kaufmann, P., Kipfstuhl, S., Kohno, M., Lambert, F., Lambrecht, A., Lambrecht, A., Landais, A., Lawer, G., Leuenberger, M., Littot, G., Loulergue, L., Lüthi, D., Maggi, V., Marino, F., Masson-Delmotte, V., Meyer, H., Miller, H., Mulvaney, R., Narcisi, B., Oerlemans, J., Oerter, H., Parrenin, F., Petit, J. R., Raisbeck, G., Raynaud, D., Röthlisberger, R., Ruth, U., Rybak, O., Severi, M., Schmitt, J., Schwander, J., Siegenthaler, U., Siggaard-Andersen, M. L., Spahni, R., Steffensen, J. P., Stenni, B., Stocker, T. F., Tison, J. L., Traversi, R., Udisti, R., Valero-Delgado, F., Van Den Broeke, M. R., Van De Wal, R. S. W., Wagenbach, D., Wegner, A., Weiler, K., Wilhelms, F., Winther, J. G., and Wolff, E.: One-to-one coupling of glacial climate variability in Greenland and Antarc-

tica, Nature, 444, 195–198, https://doi.org/10.1038/nature05301, 2006.

Bart, P. J., Krogmeier, B. J., Bart, M. P., and Tulaczyk, S.: The paradox of a long grounding during West Antarctic Ice Sheet retreat in Ross Sea, Sci. Rep., 7, 1262, https://doi.org/10.1038/s41598-017-01329-8, 2017.

Bart, P. J., DeCesare, M., Rosenheim, B. E., Majewski, W., and McGlannan, A.: A centuries-long delay between a paleo-ice-shelf collapse and grounding-line retreat in the Whales Deep Basin, eastern Ross Sea, Antarctica, Sci. Rep., 8, 1–9, https://doi.org/10.1038/s41598-018-29911-8, 2018.

Bentley, M. J., Hodgson, D. A., Smith, J. A., and Cox, N. J.: Relative sea level curves for the South Shetland Islands and Marguerite Bay, Antarctic Peninsula, Quaternary Sci. Rev., 24, 1203–1216, https://doi.org/10.1016/j.quascirev.2004.10.004, 2005.

Bentley, M. J., Fogwill, C. J., Kubik, P. W., and Sugden, D. E.: Geomorphological evidence and cosmogenic ^{10}Be/^{26}Al exposure ages for the Last Glacial Maximum and deglaciation of the Antarctic Peninsula Ice Sheet, Bull. Geol. Soc. Am., 118, 1149–1159, https://doi.org/10.1130/B25735.1, 2006.

Bentley, M. J., Fogwill, C. J., Le Brocq, A. M., Hubbard, A. L., Sugden, D. E., Dunai, T. J., and Freeman, S. P. H. T.: Deglacial history of the West Antarctic Ice Sheet in the Weddell Sea embayment: Constraints on past Ice volume change, Geology, 38, 411–414, https://doi.org/10.1130/G30754.1, 2010.

Bentley, M. J., Johnson, J. S., Hodgson, D. A., Dunai, T., Freeman, S. P. H. T., and O'Cofaigh, C.: Rapid deglaciation of Marguerite Bay, western Antarctic Peninsula in the Early Holocene, Quaternary Sci. Rev., 30, 3338–3349, https://doi.org/10.1016/j.quascirev.2011.09.002, 2011.

Bentley, M. J., Ó Cofaigh, C., Anderson, J. B., Conway, H., Davies, B., Graham, A. G. C., Hillenbrand, C.-D., Hodgson, D. A., Jamieson, S. S. R., Larter, R. D., Mackintosh, A., Smith, J. A., Verleyen, E., Ackert, R. P., Bart, P. J., Berg, S., Brunstein, D., Canals, M., Colhoun, E. a., Crosta, X., Dickens, W. a., Domack, E., Dowdeswell, J. A., Dunbar, R., Ehrmann, W., Evans, J., Favier, V., Fink, D., Fogwill, C. J., Glasser, N. F., Gohl, K., Golledge, N. R., Goodwin, I., Gore, D. B., Greenwood, S. L., Hall, B. L., Hall, K., Hedding, D. W., Hein, A. S., Hocking, E. P., Jakobsson, M., Johnson, J. S., Jomelli, V., Jones, R. S., Klages, J. P., Kristoffersen, Y., Kuhn, G., Leventer, A., Licht, K., Lilly, K., Lindow, J., Livingstone, S. J., Massé, G., McGlone, M. S., McKay, R. M., Melles, M., Miura, H., Mulvaney, R., Nel, W., Nitsche, F. O., O'Brien, P. E., Post, A. L., Roberts, S. J., Saunders, K. M., Selkirk, P. M., Simms, A. R., Spiegel, C., Stolldorf, T. D., Sugden, D. E., van der Putten, N., van Ommen, T., Verfaillie, D., Vyverman, W., Wagner, B., White, D. A., Witus, A. E., and Zwartz, D.: A community-based geological reconstruction of Antarctic Ice Sheet deglaciation since the Last Glacial Maximum, Quaternary Sci. Rev., 100, 1–9, https://doi.org/10.1016/j.quascirev.2014.06.025, 2014.

Bentley, M. J., Hein, A. S., Sugden, D. E., Whitehouse, P. L., Shanks, R., Xu, S., and Freeman, S. P. H. T.: Deglacial history of the Pensacola Mountains, Antarctica from glacial geomorphology and cosmogenic nuclide surface exposure dating, Quaternary Sci. Rev., 158, 58–76, https://doi.org/10.1016/j.quascirev.2016.09.028, 2017.

Berg, S., Wagner, B., White, D. A., and Melles, M.: No significant ice-sheet expansion beyond present ice margins during the past 4500 yr at Rauer Group, East Antarctica, Quaternary Res., 74, 23–25, https://doi.org/10.1016/j.yqres.2010.04.004, 2010.

Borchers, B., Marrero, S., Balco, G., Caffee, M., Goehring, B., Lifton, N., Nishiizumi, K., Phillips, F., Schaefer, J., and Stone, J.: Geological calibration of spallation production rates in the CRONUS-Earth project, Quat. Geochronol., 31, 188–198, https://doi.org/10.1016/j.quageo.2015.01.009, 2016.

Born, A.: Tracer transport in an isochronal ice-sheet model, J. Glaciol., 63, 22–38, https://doi.org/10.1017/jog.2016.111, 2017.

Bradley, S. L., Siddall, M., Milne, G. A., Masson-Delmotte, V., and Wolff, E.: Where might we find evidence of a Last Interglacial West Antarctic Ice Sheet collapse in Antarctic ice core records?, Global Planet. Change, 88–89, 64–75, https://doi.org/10.1016/j.gloplacha.2012.03.004, 2012.

Briggs, R. D. and Tarasov, L.: How to evaluate model-derived deglaciation chronologies: A case study using Antarctica, Quaternary Sci. Rev., 63, 109–127, https://doi.org/10.1016/j.quascirev.2012.11.021, 2013.

Briggs, R. D., Pollard, D., and Tarasov, L.: A data-constrained large ensemble analysis of Antarctic evolution since the Eemian, Quaternary Sci. Rev., 103, 91–115, https://doi.org/10.1016/j.quascirev.2014.09.003, 2014.

Buizert, C., Fudge, T. J., Roberts, W. H., Steig, E. J., Sherriff-Tadano, S., Ritz, C., Lefebvre, E., Edwards, J., Kawamura, K., Oyabu, I., and Motoyama, H.: Antarctic surface temperature and elevation during the Last Glacial Maximum, Science, 372, 1097–1101, 2021.

Cavitte, M. G. P., Young, D. A., Mulvaney, R., Ritz, C., Greenbaum, J. S., Ng, G., Kempf, S. D., Quartini, E., Muldoon, G. R., Paden, J., Frezzotti, M., Roberts, J. L., Tozer, C. R., Schroeder, D. M., and Blankenship, D. D.: A detailed radiostratigraphic data set for the central East Antarctic Plateau spanning from the Holocene to the mid-Pleistocene, Earth Syst. Sci. Data, 13, 4759–4777, https://doi.org/10.5194/essd-13-4759-2021, 2021.

Cuffey, K. M., Clow, G. D., Steig, E. J., Buizert, C., Fudge, T. J., Koutnik, M., Waddington, E. D., Alley, R. B., and Severinghaus, J. P.: Deglacial temperature history of West Antarctica, P. Natl. Acad. Sci. USA, 113, 14249–14254, https://doi.org/10.1073/pnas.1609132113, 2016.

DeConto, R. M. and Pollard, D.: Contribution of Antarctica to past and future sea-level rise, Nature, 531, 591–597, https://doi.org/10.1038/nature17145, 2016.

Delf, R., Schroeder, D. M., Curtis, A., Giannopoulos, A., and Bingham, R. G.: A comparison of automated approaches to extracting englacial-layer geometry from radar data across ice sheets, Ann. Glaciol., 61, 234–241, https://doi.org/10.1017/aog.2020.42, 2020.

Delmotte, M., Raynaud, D., Morgan, V., and Jouzel, J.: Climatic and glaciological information inferred from air-content measurements of a Law Dome (East Antarctica) ice core, J. Glaciol., 45, 255–263, https://doi.org/10.3189/s0022143000001751, 1999.

Domack, E., Duran, D., Leventer, A., Ishman, S., Doane, S., McCallum, S., Amblas, D., Ring, J., Gilbert, R., and Prentice, M.: Stability of the Larsen B ice shelf on the Antarctic Peninsula during the Holocene epoch, Nature, 436, 681–685, https://doi.org/10.1038/nature03908, 2005.

Domack, E. W., Jacobson, E. A., Shipp, S., and Anderson, J. B.: Late Pleistocene–Holocene retreat of the West Antarctic Ice-

Sheet system in the Ross Sea: Part 2 – sedimentologic and stratigraphic signature, Geol. Soc. Am. Bull., 111, 1517–1536, 1999.

Eicher, O., Baumgartner, M., Schilt, A., Schmitt, J., Schwander, J., Stocker, T. F., and Fischer, H.: Climatic and insolation control on the high-resolution total air content in the NGRIP ice core, Clim. Past, 12, 1979–1993, https://doi.org/10.5194/cp-12-1979-2016, 2016.

Ely, J. C., Clark, C. D., Small, D., and Hindmarsh, R. C. A.: ATAT 1.1, the Automated Timing Accordance Tool for comparing ice-sheet model output with geochronological data, Geosci. Model Dev., 12, 933–953, https://doi.org/10.5194/gmd-12-933-2019, 2019.

Emslie, S. D. and McDaniel, J. D.: Adelie penguin diet and climate change during the middle to late Holocene in northern Marguerite Bay, Antarctic Peninsula, Polar Biol., 25, 222–229, https://doi.org/10.1007/s00300-001-0334-y, 2002.

Engelhardt, H.: Ice temperature and high geothermal flux at Siple Dome, West Antarctica, from borehole measurements, J. Glaciol., 50, 251–256, https://doi.org/10.3189/172756504781830105, 2004a.

Engelhardt, H.: Thermal regime and dynamics of the West Antarctic ice sheet, Ann. Glaciol., 39, 85–92, https://doi.org/10.3189/172756404781814203, 2004b.

Fox-Kemper, B., Hewitt, H. T., Xiao, C., Aðalgeirsdóttir, G., Drijfhout, S. S., Edwards, T. L., Golledge, N. R., Hemer, M., Kopp, R. E., Krinner, G., Mix, A., Notz, D., Nowicki, S., Nurhati, I. S., Ruiz, L., Sallée, J.-B., Slangen, A. B. A., and Yu, Y.: Intergovernmental Panel on Climate Change. Ocean, Cryosphere and Sea Level Change, in: Climate Change 2021 – The Physical Science Basis: Working Group I Contribution to the Sixth Assessment Report of the Intergovernmental Panel on Climate Change, Cambridge University Press, Cambridge, 1211–1362, https://doi.org/10.1017/9781009157896.011, 2023.

Gasson, E., Deconto, R., and Pollard, D.: Antarctic bedrock topography uncertainty and ice sheet stability, Geophys. Res. Lett., 42, 5372–5377, https://doi.org/10.1002/2015GL064322, 2015.

Glasser, N. F., Davies, B. J., Carrivick, J. L., Rodés, A., Hambrey, M. J., Smellie, J. L., and Domack, E.: Ice-stream initiation, duration and thinning on James Ross Island, northern Antarctic Peninsula, Quaternary Sci. Rev., 86, 78–88, https://doi.org/10.1016/j.quascirev.2013.11.012, 2014.

Golledge, N. R., Menviel, L., Carter, L., Fogwill, C. J., England, M. H., Cortese, G., and Levy, R. H.: Antarctic contribution to meltwater pulse 1A from reduced Southern Ocean overturning, Nat. Commun., 5, 5107, https://doi.org/10.1038/ncomms6107, 2014.

Golledge, N. R., Kowalewski, D. E., Naish, T. R., Levy, R. H., Fogwill, C. J., and Gasson, E. G. W.: The multi-millennial Antarctic commitment to future sea-level rise, Nature, 526, 421–425, https://doi.org/10.1038/nature15706, 2015.

Gomez, N., Latychev, K., and Pollard, D.: A coupled ice sheet-sea level model incorporating 3D earth structure: Variations in Antarctica during the Last Deglacial Retreat, J. Climate, 31, 4041–4054, https://doi.org/10.1175/JCLI-D-17-0352.1, 2018.

Gow, A. J., Ueda, H. T., and Garfield, D. E.: Antarctic ice sheet: Preliminary results of first core hole to bedrock, Science, 161, 1011–1013, https://doi.org/10.1126/science.161.3845.1011, 1968.

Hall, B. L. and Denton, G. H.: New relative sea-level curves for the southern Scott Coast, Antarctica: Evidence for Holocene deglaciation of the western Ross Sea, J. Quaternary Sci., 14, 641–650, https://doi.org/10.1002/(SICI)1099-1417(199912)14:7<641::AID-JQS466>3.0.CO;2-B, 1999.

Hall, B. L., Henderson, G. M., Baroni, C., and Kellogg, T. B.: Constant Holocene Southern-Ocean ^{14}C reservoir ages and ice-shelf flow rates, Earth Planet. Sc. Lett., 296, 115–123, https://doi.org/10.1016/j.epsl.2010.04.054, 2010.

Heaton, T. J., Köhler, P., Butzin, M., Bard, E., Reimer, R. W., Austin, W. E. N., Bronk Ramsey, C., Grootes, P. M., Hughen, K. A., Kromer, B., Reimer, P. J., Adkins, J., Burke, A., Cook, M. S., Olsen, J., and Skinner, L. C.: Marine20 – The Marine Radiocarbon Age Calibration Curve (0–55 000 cal BP), Radiocarbon, 62, 779–820, https://doi.org/10.1017/RDC.2020.68, 2020.

Hein, A. S., Woodward, J., Marrero, S. M., Dunning, S. A., Steig, E. J., Freeman, S. P. H. T., Stuart, F. M., Winter, K., Westoby, M. J., and Sugden, D. E.: Evidence for the stability of the West Antarctic Ice Sheet divide for 1.4 million years, Nat. Commun., 7, 10325, https://doi.org/10.1038/ncomms10325, 2016.

Hemer, M. A. and Harris, P. T.: Sediment core from beneath the Amery Ice shelf, East Antartica, suggests mid-Holocene ice-shelf retreat, Geology, 31, 127–130, https://doi.org/10.1130/0091-7613(2003)031<0127:SCFBTA>2.0.CO;2, 2003.

Hemer, M. A., Post, A. L., O'Brien, P. E., Craven, M., Truswell, E. M., Roberts, D., and Harris, P. T.: Sedimentological signatures of the sub-Amery Ice Shelf circulation, Antarct. Sci., 19, 497–506, https://doi.org/10.1017/S0954102007000697, 2007.

Heroy, D. C. and Anderson, J. B.: Radiocarbon constraints on Antarctic Peninsula Ice Sheet retreat following the Last Glacial Maximum (LGM), Quaternary Sci. Rev., 26, 3286–3297, https://doi.org/10.1016/j.quascirev.2007.07.012, 2007.

Hillenbrand, C. D., Larter, R. D., Dowdeswell, J. A., Ehrmann, W., Ó Cofaigh, C., Benetti, S., Graham, A. G. C., and Grobe, H.: The sedimentary legacy of a palaeo-ice stream on the shelf of the southern Bellingshausen Sea: Clues to West Antarctic glacial history during the Late Quaternary, Quaternary Sci. Rev., 29, 2741–2763, https://doi.org/10.1016/j.quascirev.2010.06.028, 2010a.

Hillenbrand, C.-D., Smth, J. A., Kuhn, G., Esper, O., Gersonde, R., Larter, R. D., Maher, B., Moreton, S. G., Shimmield, T. M., and Korte, M.: Age assignment of a diatomaceous ooze deposited in the western Amundsen Sea Embayment after the Last Glacial Maximum, J. Quaternary Sci., 25, 280–295, 2010b.

Hillenbrand, C.-D., Kuhn, G., Smith, J. A., Gohl, K., Graham, A. G. C., Larter, R. D., Klages, J. P., Downey, R., Moreton, S. G., Forwick, M., and Vaughan, D. G.: Grounding-line retreat of the west Antarctic ice sheet from inner Pine island Bay, Geology, 41, 35–38, 2013.

Hillenbrand, C. D., Bentley, M. J., Stolldorf, T. D., Hein, A. S., Kuhn, G., Graham, A. G. C., Fogwill, C. J., Kristoffersen, Y., Smith, J. A., Anderson, J. B., Larter, R. D., Melles, M., Hodgson, D. A., Mulvaney, R., and Sugden, D. E.: Reconstruction of changes in the Weddell Sea sector of the Antarctic Ice Sheet since the Last Glacial Maximum, Quaternary Sci. Rev., 100, 111–136, https://doi.org/10.1016/j.quascirev.2013.07.020, 2014.

Hjort, C., Ingólfsson, Ó., Möller, P., and Lirio, J. M.: Holocene glacial history and sea-level changes on James Ross Island, Antarctic Peninsula, J. Quaternary Sci., 12, 259–273, https://doi.org/10.1002/(sici)1099-1417(199707/08)12:4<259::aid-jqs307>3.0.co;2-6, 1997.

Hodgson, D. A., Whitehouse, P. L., De Cort, G., Berg, S., Verleyen, E., Tavernier, I., Roberts, S. J., Vyverman, W., Sabbe, K., and O'Brien, P.: Rapid early Holocene sea-level rise in Prydz Bay, East Antarctica, Global Planet. Change, 139, 128–140, https://doi.org/10.1016/j.gloplacha.2015.12.020, 2016.

Hodgson, D. A., Hogan, K., Smith, J. M., Smith, J. A., Hillenbrand, C.-D., Graham, A. G. C., Fretwell, P., Allen, C., Peck, V., Arndt, J.-E., Dorschel, B., Hübscher, C., Smith, A. M., and Larter, R.: Deglaciation and future stability of the Coats Land ice margin, Antarctica, The Cryosphere, 12, 2383–2399, https://doi.org/10.5194/tc-12-2383-2018, 2018.

Huybrechts, P.: Sea-level changes at the LGM from ice-dynamic reconstructions of the Greenland and Antarctic ice sheets during the glacial cycles, Quaternary Sci. Rev., 21, 203–231, https://doi.org/10.1016/S0277-3791(01)00082-8, 2002.

Ivins, E. R., James, T. S., Wahr, J., Ernst, E. J., Landerer, F. W., and Simon, K. M.: Antarctic contribution to sea level rise observed by GRACE with improved GIA correction, J. Geophys. Res.-Sol. Ea., 118, 3126–3141, https://doi.org/10.1002/jgrb.50208, 2013.

Johnson, J. S., Bentley, M. J., and Gohl, K.: First exposure ages from the Amundsen Sea Embayment, West Antarctica: The Late quaternary context for recent thinning of Pine Island, Smith, and Pope Glaciers, Geology, 36, 223–226, https://doi.org/10.1130/G24207A.1, 2008.

Johnson, J. S., Smith, J. A., Schaefer, J. M., Young, N. E., Goehring, B. M., Hillenbrand, C. D., Lamp, J. L., Finkel, R. C., and Gohl, K.: The last glaciation of Bear Peninsula, central Amundsen Sea Embayment of Antarctica: Constraints on timing and duration revealed by in situ cosmogenic ^{14}C and ^{10}Be dating, Quaternary Sci. Rev., 178, 77–88, https://doi.org/10.1016/j.quascirev.2017.11.003, 2017.

Johnson, J. S., Nichols, K. A., Goehring, B. M., Balco, G., and Schaefer, J. M.: Abrupt mid-Holocene ice loss in the western Weddell Sea Embayment of Antarctica, Earth Planet. Sc. Lett., 518, 127–135, https://doi.org/10.1016/j.epsl.2019.05.002, 2019.

Johnson, J. S., Roberts, S. J., Rood, D. H., Pollard, D., Schaefer, J. M., Whitehouse, P. L., Ireland, L. C., Lamp, J. L., Goehring, B. M., Rand, C., and Smith, J. A.: Deglaciation of Pope Glacier implies widespread early Holocene ice sheet thinning in the Amundsen Sea sector of Antarctica, Earth Planet. Sc. Lett., 548, 116501, https://doi.org/10.1016/j.epsl.2020.116501, 2020.

Jones, R. S., Mackintosh, A. N., Norton, K. P., Golledge, N. R., Fogwill, C. J., Kubik, P. W., Christl, M., and Greenwood, S. L.: Rapid Holocene thinning of an East Antarctic outlet glacier driven by marine ice sheet instability, Nat. Commun., 6, 8910, https://doi.org/10.1038/ncomms9910, 2015.

Kingslake, J., Scherer, R. P., Albrecht, T., Coenen, J., Powell, R. D., Reese, R., Stansell, N. D., Tulaczyk, S., Wearing, M. G., and Whitehouse, P. L.: Extensive retreat and re-advance of the West Antarctic Ice Sheet during the Holocene, Nature, 558, 430–434, https://doi.org/10.1038/s41586-018-0208-x, 2018.

Kirshner, A. E., Anderson, J. B., Jakobsson, M., O'Regan, M., Majewski, W., and Nitsche, F. O.: Post-LGM deglaciation in Pine Island Bay, West Antarctica, Quaternary Sci. Rev., 38, 11–26, https://doi.org/10.1016/j.quascirev.2012.01.017, 2012.

Klages, J. P., Kuhn, G., Hillenbrand, C.-D., Graham, A. G. C., Smith, J. A., Larter, R. D., Gohl, K., and Wacker, L.: Retreat of the West Antarctic Ice Sheet from the western Amundsen Sea shelf at a pre-or early LGM stage, Quaternary Sci. Rev., 91, 1–15, 2014.

Klages, J. P., Kuhn, G., Hillenbrand, C. D., Smith, J. A., Graham, A. G. C., Nitsche, F. O., Frederichs, T., Jernas, P. E., Gohl, K., and Wacker, L.: Limited grounding-line advance onto the West Antarctic continental shelf in the easternmost Amundsen Sea Embayment during the last glacial period, PLoS One, 12, e0181593, https://doi.org/10.1371/journal.pone.0181593, 2017.

Larter, R. D., Anderson, J. B., Graham, A. G. C., Gohl, K., Hillenbrand, C. D., Jakobsson, M., Johnson, J. S., Kuhn, G., Nitsche, F. O., Smith, J. A., Witus, A. E., Bentley, M. J., Dowdeswell, J. A., Ehrmann, W., Klages, J. P., Lindow, J., Cofaigh, C. O., and Spiegel, C.: Reconstruction of changes in the Amundsen Sea and Bellingshausen Sea sector of the West Antarctic Ice Sheet since the Last Glacial Maximum, Quaternary Sci. Rev., 100, 55–86, https://doi.org/10.1016/j.quascirev.2013.10.016, 2014.

Lecavalier, B., Tarasov, L., Balco, G., Spector, P., Hillenbrand, C.-D., Buizert, C., Ritz, C., Leduc-Leballeur, M., Mulvaney, R., Whitehouse, P. L., Bentley, M. J., and Bamber, J.: Antarctic ice sheet paleo-constraint database, Ghub [data set], https://theghub.org/resources/4884, 2022.

Levermann, A., Winkelmann, R., Nowicki, S., Fastook, J. L., Frieler, K., Greve, R., Hellmer, H. H., Martin, M. A., Meinshausen, M., Mengel, M., Payne, A. J., Pollard, D., Sato, T., Timmermann, R., Wang, W. L., and Bindschadler, R. A.: Projecting Antarctic ice discharge using response functions from SeaRISE ice-sheet models, Earth Syst. Dynam., 5, 271–293, https://doi.org/10.5194/esd-5-271-2014, 2014.

Licht, K. J., Cunningham, W. L., Andrews, J. T., Domack, E. W., and Jennings, A. E.: Establishing chronologies from acid-insoluble organic ^{14}C dates on antarctic (Ross Sea) and arctic (North Atlantic) marine sediments, Polar Res., 17, 203–216, https://doi.org/10.3402/polar.v17i2.6619, 1998.

Lifton, N., Sato, T., and Dunai, T. J.: Scaling in situ cosmogenic nuclide production rates using analytical approximations to atmospheric cosmic-ray fluxes, Earth Planet. Sc. Lett., https://doi.org/10.1016/j.epsl.2013.10.052, 2014.

Little, C. M., Oppenheimer, M., and Urban, N. M.: Upper bounds on twenty-first-century Antarctic ice loss assessed using a probabilistic framework, Nat. Clim. Change, 3, 654–659, https://doi.org/10.1038/nclimate1845, 2013.

Livingstone, S. J., Ó Cofaigh, C., Stokes, C. R., Hillenbrand, C.-D., Vieli, A., and Jamieson, S. S. R.: Antarctic palaeo-ice streams, Earth Sci. Rev., 111, 90–128, https://doi.org/10.1016/j.earscirev.2011.10.003, 2012.

Lorius, C., Raynaud, D., Petit, J. R., Jouzel, J., and Merlivat, L.: Late-glacial maximum- Holocene atmospheric and ice-thickness changes from Antarctic ice-core studies, Ann. Glaciol., 5, 88–94, https://doi.org/10.3189/1984aog5-1-88-94, 1984.

Lukin, V. V. and Vasiliev, N. I.: Technological aspects of the final phase of drilling borehole 5G and unsealing Vostok Subglacial Lake, East Antarctica, Ann. Glaciol., 55, 83–89, https://doi.org/10.3189/2014AoG65A002, 2014.

MacGregor, J. A., Fahnestock, M. A., Catania, G. A., Paden, J. D., Prasad Gogineni, S., Young, S. K., Rybarski, S. C., Mabrey, A. N., Wagman, B. M., and Morlighem, M.: Radiostratigraphy and age structure of the Greenland Ice Sheet, J. Geophys. Res.-Earth, 120, 212–241, https://doi.org/10.1002/2014JF003215, 2015.

Mackintosh, A., White, D., Fink, D., Gore, D. B., Pickard, J., and Fanning, P. C.: Exposure ages from mountain dipsticks in Mac. Robertson Land, East Antarctica, indicate little change in ice-sheet thickness since the Last Glacial Maximum, Geology, 35, 551–554, https://doi.org/10.1130/G23503A.1, 2007.

Mackintosh, A. N., Verleyen, E., O'Brien, P. E., White, D. A., Jones, R. S., McKay, R., Dunbar, R., Gore, D. B., Fink, D., Post, A. L., and Miura, H.: Retreat history of the East Antarctic Ice Sheet since the last glacial maximum, Quaternary Sci. Rev., 100, 10–30, 2014.

Martín-Español, A., Zammit-Mangion, A., Clarke, P. J., Flament, T., Helm, V., King, M. A., Luthcke, S. B., Petrie, E., Rémy, F., Schön, N., Wouters, B., and Bamber, J. L.: Spatial and temporal Antarctic Ice Sheet mass trends, glacio-isostatic adjustment, and surface processes from a joint inversion of satellite altimeter, gravity, and GPS data, J. Geophys. Res.-Earth, 121, 182–200, https://doi.org/10.1002/2015JF003550, 2016.

Mas e Braga, M., Selwyn Jones, R., Newall, J. C. H., Rogozhina, I., Andersen, J. L., Lifton, N. A., and Stroeven, A. P.: Nunataks as barriers to ice flow: implications for palaeo ice sheet reconstructions, The Cryosphere, 15, 4929–4947, https://doi.org/10.5194/tc-15-4929-2021, 2021.

Matsuoka, K., Skoglund, A., Roth, G., de Pomereu, J., Griffiths, H., Headland, R., Herried, B., Katsumata, K., le Brocq, A., Licht, K., Morgan, F., Neff, P. D., Ritz, C., Scheinert, M., Tamura, T., van de Putte, A., van den Broeke, M., von Deschwanden, A., Deschamps-Berger, C., Liefferinge, B. van, Tronstad, S., and Melvaer, Y.: Quantarctica, an integrated mapping environment for Antarctica, the Southern Ocean, and sub-Antarctic islands, Environ. Modell. Softw., 140, 105015, https://doi.org/10.21334/npolar.2018.8516e961, 2021.

McGlannan, A. J., Bart, P. J., Chow, J. M., and DeCesare, M.: On the influence of post-LGM ice shelf loss and grounding zone sedimentation on West Antarctic ice sheet stability, Mar. Geol., 392, 151–169, https://doi.org/10.1016/j.margeo.2017.08.005, 2017.

McKay, R. M., Dunbar, G. B., Naish, T. R., Barrett, P. J., Carter, L., and Harper, M.: Retreat history of the Ross Ice Sheet (Shelf) since the Last Glacial Maximum from deep-basin sediment cores around Ross Island, Palaeogeogr. Palaeocl., 260, 245–261, https://doi.org/10.1016/j.palaeo.2007.08.015, 2008.

McKay, R., Golledge, N. R., Maas, S., Naish, T., Levy, R., Dunbar, G., and Kuhn, G.: Antarctic marine ice-sheet retreat in the Ross Sea during the early Holocene, Geology, 44, 7–10, 2016.

Meredith, M., Sommerkorn, M., Cassotta, S., Derksen, C., Ekaykin, A., Hollowed, A., Kofinas, G., Mackintosh, A., Melbourne-Thomas, J., Muelbert, M. M. C., Ottersen, G., Pritchard, H., and Schuur, E. A. G.: Polar Regions, in: IPCC Special Report on the Ocean and Cryosphere in a Changing Climate, IPCC, https://doi.org/10.1017/9781009157964.005, 2019.

Miura, H., Moriwaki, K., Maemoku, H., and Hirakawa, K.: Fluctuations of the East Antarctic ice-sheet margin since the last glaciation from the stratigraphy of raised beach deposits along the Soya Coast, Ann. Glaciol., 27, 297–301, 1998.

Morlighem, M., Rignot, E., Binder, T., Blankenship, D., Drews, R., Eagles, G., Eisen, O., Ferraccioli, F., Forsberg, R., Fretwell, P., Goel, V., Greenbaum, J. S., Gudmundsson, H., Guo, J., Helm, V., Hofstede, C., Howat, I., Humbert, A., Jokat, W., Karlsson, N. B., Lee, W. S., Matsuoka, K., Millan, R., Mouginot, J., Paden, J., Pattyn, F., Roberts, J., Rosier, S., Ruppel, A., Seroussi,

H., Smith, E. C., Steinhage, D., Sun, B., van den Broeke, M. R., van Ommen, T. D., van Wessem, M., and Young, D. A.: Deep glacial troughs and stabilizing ridges unveiled beneath the margins of the Antarctic ice sheet, Nat. Geosci., 13, 132–137, https://doi.org/10.1038/s41561-019-0510-8, 2020.

Motoyama, H.: The Second Deep Ice Coring Project at Dome Fuji, Antarctica, Sci. Dril., 5, 41–43, https://doi.org/10.2204/iodp.sd.5.05.2007, 2007.

Mouginot, J., Rignot, E., and Scheuchl, B.: Continent-Wide, Interferometric SAR Phase, Mapping of Antarctic Ice Velocity, Geophys. Res. Lett., 46, 9710–9718, https://doi.org/10.1029/2019GL083826, 2019.

Mulvaney, R., Rix, J., Polfrey, S., Grieman, M., Martìn, C., Nehrbass-Ahles, C., Rowell, I., Tuckwell, R., and Wolff, E.: Ice drilling on Skytrain Ice Rise and Sherman Island, Antarctica, Ann. Glaciol., 62, 311–323, https://doi.org/10.1017/aog.2021.7, 2021.

Neuhaus, S. U., Tulaczyk, S. M., Stansell, N. D., Coenen, J. J., Scherer, R. P., Mikucki, J. A., and Powell, R. D.: Did Holocene climate changes drive West Antarctic grounding line retreat and readvance?, The Cryosphere, 15, 4655–4673, https://doi.org/10.5194/tc-15-4655-2021, 2021.

Neumann, T. A., Conways, H., Price, S. F., Waddington, E. D., Catania, G. A., and Morse, D. L.: Holocene accumulation and ice sheet dynamics in central West Antarctica, J. Geophys. Res.-Earth, 113, 1–9, https://doi.org/10.1029/2007JF000764, 2008.

Nichols, K. A., Goehring, B. M., Balco, G., Johnson, J. S., Hein, A. S., and Todd, C.: New Last Glacial Maximum ice thickness constraints for the Weddell Sea Embayment, Antarctica, The Cryosphere, 13, 2935–2951, https://doi.org/10.5194/tc-13-2935-2019, 2019.

Ó Cofaigh, C., Davies, B. J., Livingstone, S. J., Smith, J. A., Johnson, J. S., Hocking, E. P., Hodgson, D. A., Anderson, J. B., Bentley, M. J., Canals, M., Domack, E., Dowdeswell, J. A., Evans, J., Glasser, N. F., Hillenbrand, C.-D., Larter, R. D., Roberts, S. J., and Simms, A. R.: Reconstruction of ice-sheet changes in the Antarctic Peninsula since the Last Glacial Maximum, Quaternary Sci. Rev., 100, 87–110, https://doi.org/10.1016/j.quascirev.2014.06.023, 2014.

Ohkouchi, N. and Eglinton, T. I.: Compound-specific radiocarbon dating of Ross Sea sediments: A prospect for constructing chronologies in high-latitude oceanic sediments, Quat. Geochronol., 3, 235–243, https://doi.org/10.1016/j.quageo.2007.11.001, 2008.

Parrenin, F., Barnola, J.-M., Beer, J., Blunier, T., Castellano, E., Chappellaz, J., Dreyfus, G., Fischer, H., Fujita, S., Jouzel, J., Kawamura, K., Lemieux-Dudon, B., Loulergue, L., Masson-Delmotte, V., Narcisi, B., Petit, J.-R., Raisbeck, G., Raynaud, D., Ruth, U., Schwander, J., Severi, M., Spahni, R., Steffensen, J. P., Svensson, A., Udisti, R., Waelbroeck, C., and Wolff, E.: The EDC3 chronology for the EPICA Dome C ice core, Clim. Past, 3, 485–497, https://doi.org/10.5194/cp-3-485-2007, 2007.

Pollard, D. and DeConto, R. M.: Modelling West Antarctic ice sheet growth and collapse through the past five million years, Nature, 458, 329–332, https://doi.org/10.1038/nature07809, 2009.

Post, A. L., Hemer, M. A., O'Brien, P. E., Roberts, D., and Craven, M.: History of benthic colonisation beneath the Amery Ice Shelf, East Antarctica, Mar. Ecol. Prog. Ser., 344, 29–37, https://doi.org/10.3354/meps06966, 2007.

Post, A. L., Galton-Fenzi, B. K., Riddle, M. J., Herraiz-Borreguero, L., O'Brien, P. E., Hemer, M. A., McMinn, A., Rasch, D., and Craven, M.: Modern sedimentation, circulation and life beneath the Amery Ice Shelf, East Antarctica, Cont. Shelf Res., 74, 77–87, https://doi.org/10.1016/j.csr.2013.10.010, 2014.

Pudsey, C. J., Murray, J. W., Appleby, P., and Evans, J.: Ice shelf history from petrographic and foraminiferal evidence, Northeast Antarctic Peninsula, Quaternary Sci. Rev., 25, 2357–2379, https://doi.org/10.1016/j.quascirev.2006.01.029, 2006.

Raynaud, D., Lipenkov, V., Lemieux-Dudon, B., Duval, P., Loutre, M. F., and Lhomme, N.: The local insolation signature of air content in Antarctic ice. A new step toward an absolute dating of ice records, Earth Planet. Sc. Lett., 261, 337–349, https://doi.org/10.1016/j.epsl.2007.06.025, 2007.

Reimer, P. J., Baillie, M. G. L., Bard, E., Bayliss, A., Beck, J. W., Blackwell, P. G., Bronk Ramsey, C., Buck, C. E., Burr, G. S., Edwards, R. L., Friedrich, M., Grootes, P. M., Guilderson, T. P., Hajdas, I., Heaton, T. J., Hogg, A. G., Hughen, K. A., Kaiser, K. F., Kromer, B., McCormac, F. G., Manning, S. W., Reimer, R. W., Richards, D. A., Southon, J. R., Talamo, S., Turney, C. S. M., van der Plicht, J., and Weyhenmeyer, C. E.: INTCAL 09 and MARINE09 aadiocarbon age calibration curves, 0–50 000 years Cal BP, Radiocarbon, 51, 1111–1150, https://doi.org/10.2458/azu_js_rc.51.3569, 2009.

Riddle, M. J., Craven, M., Goldsworthy, P. M., and Carsey, F.: A diverse benthic assemblage 100 km from open water under the Amery Ice Shelf, Antarctica, Paleoceanography, 22, PA1204, https://doi.org/10.1029/2006PA001327, 2007.

Ritz, C., Edwards, T. L., Durand, G., Payne, A. J., Peyaud, V., and Hindmarsh, R. C. A.: Potential sea-level rise from Antarctic ice-sheet instability constrained by observations, Nature, 528, 115–118, https://doi.org/10.1038/nature16147, 2015.

Roberts, S. J., Hodgson, D. A., Sterken, M., Whitehouse, P. L., Verleyen, E., Vyverman, W., Sabbe, K., Balbo, A., Bentley, M. J., and Moreton, S. G.: Geological constraints on glacio-isostatic adjustment models of relative sea-level change during deglaciation of Prince Gustav Channel, Antarctic Peninsula, Quaternary Sci. Rev., 30, 3603–3617, https://doi.org/10.1016/j.quascirev.2011.09.009, 2011.

Rosenheim, B. E., Day, M. B., Domack, E., Schrum, H., Benthien, A., and Hayes, J. M.: Antarctic sediment chronology by programmed-temperature pyrolysis: Methodology and data treatment, Geochem. Geophy. Geosy., 9, Q04005, https://doi.org/10.1029/2007GC001816, 2008.

Ruckert, K. L., Shaffer, G., Pollard, D., Guan, Y., Wong, T. E., Forest, C. E., and Keller, K.: Assessing the impact of retreat mechanisms in a simple antarctic ice sheet model using Bayesian calibration, PLoS One, 12, 1–15, https://doi.org/10.1371/journal.pone.0170052, 2017.

Sasgen, I., Martín-Español, A., Horvath, A., Klemann, V., Petrie, E. J., Wouters, B., Horwath, M., Pail, R., Bamber, J. L., Clarke, P. J., Konrad, H., and Drinkwater, M. R.: Joint inversion estimate of regional glacial isostatic adjustment in Antarctica considering a lateral varying Earth structure (ESA STSE Project REGINA), Geophys. J. Int., 211, 1534–1553, https://doi.org/10.1093/gji/ggx368, 2017.

Shennan, I., Long, A. J., and Horton, B. P.: Handbook of Sea-Level Research, John Wiley & Sons Ltd., https://doi.org/10.1002/9781118452547, 2015.

Shepherd, A., Ivins, E., Rignot, E., Smith, B., Van Den Broeke, M., Velicogna, I., Whitehouse, P., Briggs, K., Joughin, I., Krinner, G., Nowicki, S., Payne, T., Scambos, T., Schlegel, N., Geruo, A., Agosta, C., Ahlstrøm, A., Babonis, G., Barletta, V., Blazquez, A., Bonin, J., Csatho, B., Cullather, R., Felikson, D., Fettweis, X., Forsberg, R., Gallee, H., Gardner, A., Gilbert, L., Groh, A., Gunter, B., Hanna, E., Harig, C., Helm, V., Horvath, A., Horwath, M., Khan, S., Kjeldsen, K. K., Konrad, H., Langen, P., Lecavalier, B., Loomis, B., Luthcke, S., McMillan, M., Melini, D., Mernild, S., Mohajerani, Y., Moore, P., Mouginot, J., Moyano, G., Muir, A., Nagler, T., Nield, G., Nilsson, J., Noel, B., Otosaka, I., Pattle, M. E., Peltier, W. R., Pie, N., Rietbroek, R., Rott, H., Sandberg-Sørensen, L., Sasgen, I., Save, H., Scheuchl, B., Schrama, E., Schröder, L., Seo, K. W., Simonsen, S., Slater, T., Spada, G., Sutterley, T., Talpe, M., Tarasov, L., Van De Berg, W. J., Van Der Wal, W., Van Wessem, M., Vishwakarma, B. D., Wiese, D., and Wouters, B.: Mass balance of the Antarctic Ice Sheet from 1992 to 2017, Nature, 558, 219–222, https://doi.org/10.1038/s41586-018-0179-y, 2018.

Simkins, L. M., Simms, A. R., and DeWitt, R.: Relative sea-level history of Marguerite Bay, Antarctic Peninsula derived from optically stimulated luminescence-dated beach cobbles, Quaternary Sci. Rev., 77, 141–155, https://doi.org/10.1016/j.quascirev.2013.07.027, 2013.

Simms, A. R., Milliken, K. T., Anderson, J. B., and Wellner, J. S.: The marine record of deglaciation of the South Shetland Islands, Antarctica since the Last Glacial Maximum, Quaternary Sci. Rev., 30, 1583–1601, 2011.

Simms, A. R., Lisiecki, L., Gebbie, G., Whitehouse, P. L., and Clark, J. F.: Balancing the last glacial maximum (LGM) sea-level budget, Quaternary Sci. Rev., 205, 143–153, https://doi.org/10.1016/j.quascirev.2018.12.018, 2019.

Small, D., Bentley, M. J., Jones, R. S., Pittard, M. L., and Whitehouse, P. L.: Antarctic ice sheet palaeo-thinning rates from vertical transects of cosmogenic exposure ages, Quaternary Sci. Rev., 206, 65–80, https://doi.org/10.1016/j.quascirev.2018.12.024, 2019.

Smith, J. A., Hillenbrand, C. D., Kuhn, G., Larter, R. D., Graham, A. G. C., Ehrmann, W., Moreton, S. G., and Forwick, M.: Deglacial history of the West Antarctic Ice Sheet in the western Amundsen Sea Embayment, Quaternary Sci. Rev., 30, 488–505, https://doi.org/10.1016/j.quascirev.2010.11.020, 2011.

Smith, J. A., Hillenbrand, C. D., Kuhn, G., Klages, J. P., Graham, A. G. C., Larter, R. D., Ehrmann, W., Moreton, S. G., Wiers, S., and Frederichs, T.: New constraints on the timing of West Antarctic Ice Sheet retreat in the eastern Amundsen Sea since the Last Glacial Maximum, Global Planet. Change, 122, 224–237, https://doi.org/10.1016/j.gloplacha.2014.07.015, 2014.

Smith, J. A., Graham, A. G. C., Post, A. L., Hillenbrand, C. D., Bart, P. J., and Powell, R. D.: The marine geological imprint of Antarctic ice shelves, Nat. Commun., 10, 5635, https://doi.org/10.1038/s41467-019-13496-5, 2019.

Smith, J. A., Hillenbrand, C. D., Subt, C., Rosenheim, B. E., Frederichs, T., Ehrmann, W., Andersen, T. J., Wacker, L., Makinson, K., Anker, P., Venables, E. J., and Nicholls, K. W.: History of the Larsen C Ice Shelf reconstructed from sub–ice shelf and offshore sediments, Geology, 49, 978–982, https://doi.org/10.1130/G48503.1, 2021.

Spector, P., Stone, J., Cowdery, S. G., Hall, B., Conway, H., and Bromley, G.: Rapid early-Holocene deglaciation in the Ross Sea, Antarctica, Geophys. Res. Lett., 44, 7817–7825, https://doi.org/10.1002/2017GL074216, 2017.

Steig, E., Fastook, J., Zweck, C., Goodwin, I., Licht, K., White, J., and Ackert Jr., R. P.: West Antarctic ice sheet elevation changes, The West Antarctic Ice Sheet: Behaviour and Environment, Antar. Res. S., 77, 75–90, 2001.

Stolldorf, T., Schenke, H.-W., and Anderson, J. B.: LGM ice sheet extent in the Weddell Sea: evidence for diachronous behavior of Antarctic Ice Sheets, Quaternary Sci. Rev., 48, 20–31, 2012.

Stone, J. O. H., Balco, G. A., Sugden, D. E., Caffee, M. W., Sass, L. C., Cowdery, S. G., and Siddoway, C.: Holocene deglaciation of Marie Byrd Land, West Antarctica, Science, 299, 99–102, https://doi.org/10.1126/science.1077998, 2003.

Storey, B. C., Fink, D., Hood, D., Joy, K., Shulmeister, J., Riger-Kusk, M., and Stevens, M. I.: Cosmogenic nuclide exposure age constraints on the glacial history of the Lake Wellman area, Darwin Mountains, Antarctica, Antarct. Sci., 22, 603–618, https://doi.org/10.1017/S0954102010000799, 2010.

Stuiver, M. and Reimer, P. J.: Extended ^{14}C data base and revised CALIB 3.0 ^{14}C age calibration program, Radiocarbon, 35, 215–230, https://doi.org/10.1017/S0033822200013904, 1993.

Subt, C., Yoon, H. I., Yoo, K. C., Lee, J. I., Leventer, A., Domack, E. W., and Rosenheim, B. E.: Sub-ice shelf sediment geochronology utilizing novel radiocarbon methodology for highly detrital sediments, Geochem. Geophy. Geosy., 18, 1404–1418, https://doi.org/10.1002/2016GC006578, 2017.

Suganuma, Y., Miura, H., Zondervan, A., and Okuno, J.: East Antarctic deglaciation and the link to global cooling during the Quaternary: Evidence from glacial geomorphology and ^{10}Be surface exposure dating of the Sør Rondane Mountains, Dronning Maud Land, Quaternary Sci. Rev., 97, 102–120, https://doi.org/10.1016/j.quascirev.2014.05.007, 2014.

Sun, S., Cornford, S. L., Liu, Y., and Moore, J. C.: Dynamic response of Antarctic ice shelves to bedrock uncertainty, The Cryosphere, 8, 1561–1576, https://doi.org/10.5194/tc-8-1561-2014, 2014.

Sun, W., Zhou, X., Zhou, D., and Sun, Y.: Advances and Accuracy Assessment of Ocean Tide Models in the Antarctic Ocean, Front. Earth Sci., 10, 757821, https://doi.org/10.3389/feart.2022.757821, 2022.

Sutter, J., Fischer, H., and Eisen, O.: Investigating the internal structure of the Antarctic ice sheet: the utility of isochrones for spatiotemporal ice-sheet model calibration, The Cryosphere, 15, 3839–3860, https://doi.org/10.5194/tc-15-3839-2021, 2021.

Tarasov, L. and Goldstein, M.: Assessing uncertainty in past ice and climate evolution: overview, stepping-stones, and challenges, Clim. Past Discuss. [preprint], https://doi.org/10.5194/cp-2021-145, 2021.

Todd, C., Stone, J., Conway, H., Hall, B., and Bromley, G.: Late Quaternary evolution of Reedy Glacier, Antarctica, Quaternary Sci. Rev., 29, 1328–1341, https://doi.org/10.1016/j.quascirev.2010.02.001, 2010.

Van Ommen, T. D., Morgan, V. I., Jacka, T. H., Woon, S., and Elcheikh, A.: Near-surface temperatures in the Dome Summit South (Law Dome, East Antarctica) borehole, Ann. Glaciol., 29, 141–144, https://doi.org/10.3189/172756499781821382, 1999.

Verleyen, E., Hodgson, D. A., Milne, G. A., Sabbe, K., and Vyverman, W.: Relative sea-level history from the Lambert Glacier region, East Antarctica, and its relation to deglaciation and Holocene glacier readvance, Quaternary Res., 63, 45–52, https://doi.org/10.1016/j.yqres.2004.09.005, 2005.

Verleyen, E., Tavernier, I., Hodgson, D. A., Whitehouse, P. L., Kudoh, S., Imura, S., Heirman, K., Bentley, M. J., Roberts, S. J., De Batist, M., Sabbe, K., and Vyverman, W.: Ice sheet retreat and glacio-isostatic adjustment in Lützow-Holm Bay, East Antarctica, Quaternary Sci. Rev., 169, 85–98, https://doi.org/10.1016/j.quascirev.2017.06.003, 2017.

Waddington, E. D., Conway, H., Steig, E. J., Alley, R. B., Brook, E. J., Taylor, K. C., and White, J. W. C.: Decoding the dipstick: Thickness of Siple Dome, West Antarctica, at the Last Glacial Maximum, Geology, 33, 281–284, https://doi.org/10.1130/G21165.1, 2005.

Watcham, E. P., Bentley, M. J., Hodgson, D. A., Roberts, S. J., Fretwell, P. T., Lloyd, J. M., Larter, R. D., Whitehouse, P. L., Leng, M. J., Monien, P., and Moreton, S. G.: A new Holocene relative sea level curve for the South Shetland Islands, Antarctica, Quaternary Sci. Rev., 30, 3152–3170, https://doi.org/10.1016/j.quascirev.2011.07.021, 2011.

Weikusat, I., Jansen, D., Binder, T., Eichler, J., Faria, S. H., Wilhelms, F., Kipfstuhl, S., Sheldon, S., Miller, H., Dahl-Jensen, D., and Kleiner, T.: Physical analysis of an Antarctic ice core-towards an integration of micro-and macrodynamics of polar ice, Philos. T. R. Soc. A, 375, 20150347, https://doi.org/10.1098/rsta.2015.0347, 2017.

Whitehouse, P. L., Bentley, M. J., and Le Brocq, A. M.: A deglacial model for Antarctica: Geological constraints and glaciological modelling as a basis for a new model of Antarctic glacial isostatic adjustment, Quaternary Sci. Rev., 32, 1–24, https://doi.org/10.1016/j.quascirev.2011.11.016, 2012a.

Whitehouse, P. L., Bentley, M. J., Milne, G. A., King, M. A., and Thomas, I. D.: A new glacial isostatic adjustment model for Antarctica: calibrated and tested using observations of relative sea-level change and present-day uplift rates, Geophys. J. Int., 190, 1464–1482, https://doi.org/10.1111/j.1365-246X.2012.05557.x, 2012b.

Whitehouse, P. L., Gomez, N., King, M. A., and Wiens, D. A.: Solid Earth change and the evolution of the Antarctic Ice Sheet, Nat. Commun., 10, 1–14, https://doi.org/10.1038/s41467-018-08068-y, 2019.

Winter, A., Steinhage, D., Creyts, T. T., Kleiner, T., and Eisen, O.: Age stratigraphy in the East Antarctic Ice Sheet inferred from radio-echo sounding horizons, Earth Syst. Sci. Data, 11, 1069–1081, https://doi.org/10.5194/essd-11-1069-2019, 2019.

Yokoyama, Y., Anderson, J. B., Yamane, M., Simkins, L. M., Miyairi, Y., Yamazaki, T., Koizumi, M., Suga, H., Kusahara, K., Prothro, L., Hasumi, H., Southon, J. R., and Ohkouchi, N.: Widespread collapse of the Ross Ice Shelf during the late Holocene, P. Natl. Acad. Sci. USA, 113, 2354–2359, https://doi.org/10.1073/pnas.1516908113, 2016.

Zwartz, D., Bird, M., Stone, J., and Lambeck, K.: Holocene sea-level change and ice-sheet history in the Vestfold Hills, East Antarctica, Earth Planet. Sc. Lett., 155, 131–145, https://doi.org/10.1016/S0012-821X(97)00204-5, 1998.